Bedrijfstakonderzoek
BTO 2024.009| January 2024

AI-based reversible membrane fouling early warning system for Ultrafiltration

Proof-of-concept

Bedrijfstakonderzoek

KWR

Bridging Science to Practice

Report

AI-based reversible membrane fouling early warning system for Ultrafiltration
Proof-of-concept

BTO 2024.009| January 2024

This research is part of the Joint Research Programme of KWR, the water utilities and Vewin.

Project number
402045/279

Project manager
Ron Jong/Martijn van Veggel

Client
BTO – Bedrijfsonderzoek partners: PWN, Evides and Dunea

Author(s)
Julian Munoz Sierra, Siddharth Seshan, Luuk de Waal, Bas Wols, Maria Lousada-Ferreira

Quality Assurance
Emile Cornelissen

Sent to

This report is distributed to BTO-participants. It also summarized the results and conclusions obtained from the project "Seasonal Effects of surface water on UF fouling potential" (402045/222) in the sections entitled "Screening of water quality parameters to predict fouling".
A year after publication it is public.

Keywords
Ultrafiltration, backwash, transmembrane pressure, early warning, neural networks

Year of publishing
2024

More information
Dr.EngD.ir. Julian Muñoz Sierra
T +31 6 52891321
E julian.munoz@kwrwater.nl

PO Box 1072
3430 BB Nieuwegein
The Netherlands

T +31 (0)30 60 69 511
E info@kwrwater.nl
I www.kwrwater.nl

Managementsamenvatting

AI-gebaseerd vroegtijdig waarschuwingssysteem voor membraanvervuiling tijdens ultrafiltratie: Proof of concept

Auteur(s) Julian Munoz Sierra, Siddharth Seshan, Luuk de Waal, Bas Wols, Maria Lousada-Ferreira

AI-modellen kunnen bijdragen aan betere voorspelling van de vervuiling van ultrafiltratiemembranen. Gekeken is naar effectievere benaderingen om de prestaties van membraanprocessen nauwkeurig te kunnen voorspellen en de ontwikkeling van een proof of concept voor een vroegtijdig waarschuwingssysteem dat ontworpen is om vervuilingsgedrag te voorspellen, in het bijzonder de toename in transmembraandruk, binnen full-scale Ultrafiltratie (UF) membraaninstallaties. Een met historische data getraind AI-model blijkt in staat om de vervuiling in een specifieke installatie te voorspellen, maar is nog niet gegeneraliseerd genoeg om ook goede voorspellingen te doen voor andere UF-installaties. Aanbevelingen voor geschikte parameters, verdere dataverzameling en aanvullende modeltraining zijn geformuleerd, evenals voor de ontwikkeling van hybride modellen die de inzet van het vroegtijdig waarschuwingssysteem in volle schaal systemen kunnen stimuleren.

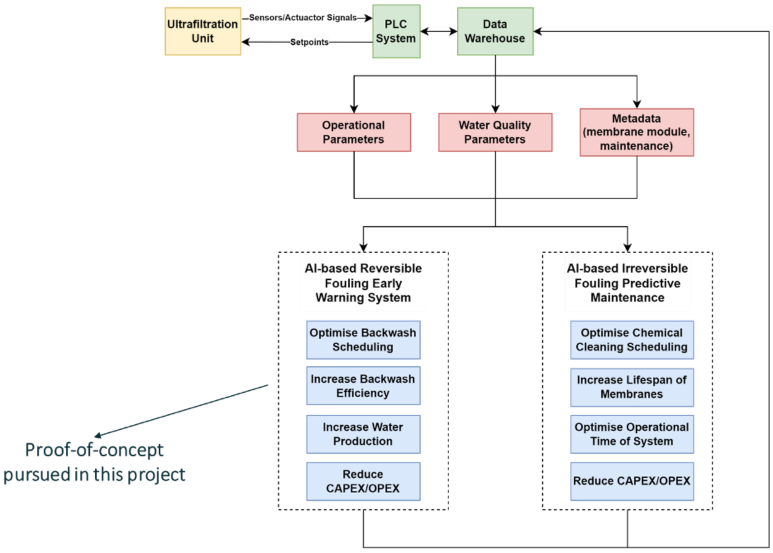

Beoogd vroegtijdig waarschuwingssysteem en voorspellend onderhoudskader voor de werking van UF-membraansystemen op basis van AI-voorspellingsmodellen. Aangegeven staat voor welk onderdeel een Proof of Concept is gezocht in dit project.

Belang: De prestaties van complexe membraanprocessen beter voorspellen

Membraanvervuilingsprocessen zijn complex en het is een hele uitdaging om het ontstaan of de ontwikkeling van membraanvervuiling nauwkeurig te voorspellen met klassieke mechanistische wiskundige modellen. De snelle ontwikkeling van kunstmatige intelligentie (AI) biedt een grote kans om effectievere benaderingen te ontwikkelen om de prestaties van membraanprocessen nauwkeurig te voorspellen. Innovatie en ontwikkeling op AI-gebied bieden mogelijkheden voor meer systeemefficiëntie, prestatievoorspelling op lange termijn en integratie van AI-strategieën in werkende systemen. AI biedt leervermogen en kan omgaan met onnauwkeurige en zeer complexe niet-lineaire gegevens en zo membraanvervuiling voorspellen door te leren uit datasets in plaats van wiskundige vergelijkingen te gebruiken.

Aanpak: neurale netwerkmodellen gevoed met historische data, laboratorium en full-scale

Onze aanpak maakt gebruik van kunstmatige intelligentie (AI) met datagestuurde methoden, waarbij neurale netwerkmodellen worden gebruikt die zijn getraind met gegevens uit full-scale installaties. Deze modellen worden ontwikkeld om prestaties te voorspellen. Zij worden gevoed met historische gegevens over de waterkwaliteit en de werking van de installatie. Na het identificeren van optimale modellen voor het voorspellen van de transmembraandruk (TMP) op korte termijn, wordt hun vermogen voor recursieve voorspellingen over een langere horizon beoordeeld. AI-modellen worden getraind door middel van uitgebreide voorbewerking van gegevens en feature engineering, waaronder een halfautomatische methode voor TMP-cyclus- en terugspoelgebeurtenisidentificatie. Het primaire doel is om de onderliggende processen te begrijpen en TMP-waarden te voorspellen voor toekomstige filtratiecycli. De modellen zijn getest op verschillende waterbronnen, onder meer met mini-ultrafiltratietests, om te evalueren of wat ze leren over membraanvervuiling zo algemeen inzetbaar is dat ze nauwkeurige voorspellingen kunnen doen voor verschillende ultrafiltratiesystemen.

Resultaten: AI-modellen voorspellen stijging van TMP tijdens opeenvolgende filtratiecycli
De getrainde neurale netwerkmodellen konden de initiële en uiteindelijke TMP-waarden tot 3 filtratiecycli vooruit voorspellen op basis van gegevens over waterkwaliteit en operationele parameters. Dit resulteerde in zeer nauwkeurige voorspellingen met R2-waarden van meer dan 0,95. Deze resultaten suggereren dat de toegepaste aanpak voor het voorbewerken van gegevens en het modelleren met neurale netwerken veelbelovend is voor het voorspellen van de toename in TMP tijdens de volgende filtratiecycli. De modellen kunnen dus dienen als een effectief waarschuwingssysteem voor de UF-installatie in Heemskerk.

Toen datasets van een ander UF-systeem (UF pilot Valkenburgse meer van Dunea) werden ingevoerd in de modellen, bleken die significant slechte prestaties te leveren bij het voorspellen van 1 filtratiecyclus vooruit – de modellen zijn niet gegeneraliseerd genoeg om op andere installaties toe te passen.

In mini-ultrafiltratietests werden de correlaties tussen waterkwaliteitsparameters en membraanweerstand onderzocht, waarbij significante variaties werden gevonden op basis van watertype/locatie. Geschikte parameters voor een potentieel vroegtijdig waarschuwingssysteem zijn biopolymeren, MFI-45, SAC, Mn, MFI-UF en troebelheid, waarbij SAC en MFI-UF een sterke correlatie vertoonden met niet-terugspoelbare weerstand. SAC wordt aanbevolen voor monitoring op volle schaal. De studie maakt gebruik van machine learning, waarbij SAC-gegevens worden gebruikt om de transmembraandruk in een volledige UF-fabriek (Heemskerk) te voorspellen. Het datagestuurde model benadrukt het belang van SAC bij het verklaren en voorspellen van volledige UF-membraanvervuiling, wat het potentieel voor verbeterde modellering suggereert.

Toepassing: AI-modellen kunnen vervuiling membranen voorspellen, verdere ontwikkeling
De resultaten van het onderzoek bieden waardevolle inzichten in het potentieel van op AI gebaseerde methodologieën voor het trainen van datagestuurde modellen als een vroegtijdig waarschuwingssysteem om te anticiperen op membraanvervuiling in UF-systemen. De onderzochte methodologieën kunnen verder worden ontwikkeld en gebruikt voor geavanceerde operationele begeleiding zoals het optimaliseren van terugspoelintervallen en reinigingsintervallen en het bijbehorende chemicaliënverbruik. Ook kunnen ze aanzienlijk bijdragen aan de voorzieningszekerheid in UF-membraaninstallaties en een robuuster waterzuiveringssysteem. Er is potentieel voor toepassing en training in andere UF-installaties in de toekomst. Het project heeft gerichte aanbevelingen opgeleverd voor verdere dataverzameling, suggesties voor aanvullende modeltraining en voor de ontwikkeling van hybride modellen die de inzet van het vroegtijdig waarschuwingssysteem in volle schaal systemen kunnen stimuleren.

Rapport
Dit onderzoek wordt gerapporteerd in het rapport *AI-gebaseerd omkeerbaar membraanvervuilings-systeem voor ultrafiltratie* (BTO 2024.009).

Management summary

AI-based reversible membrane fouling early warning system for Ultrafiltration: Proof of concept

Author(s) Julian Munoz Sierra, Siddharth Seshan, Luuk de Waal, Bas Wols, Maria Lousada-Ferreira.
Due to the complexity of membrane fouling processes, it is rather challenging to accurately predict the occurrence or evolution of membrane fouling using these classical mechanistic mathematical models. Therefore, it is very necessary to develop more effective approaches that can accurately predict the performance of membrane processes. The rapid development of artificial intelligence (AI) offers a great opportunity to achieve this goal. In this project, we propose the development of a proof of concept for an early warning system designed to predict fouling behavior, specifically the increase in transmembrane pressure, within full-scale Ultrafiltration (UF) membrane plants. The primary objective for water companies is to create a forecasting tool capable of predicting surface water fouling potential based on operational historical data and real-time support from water quality online monitoring.

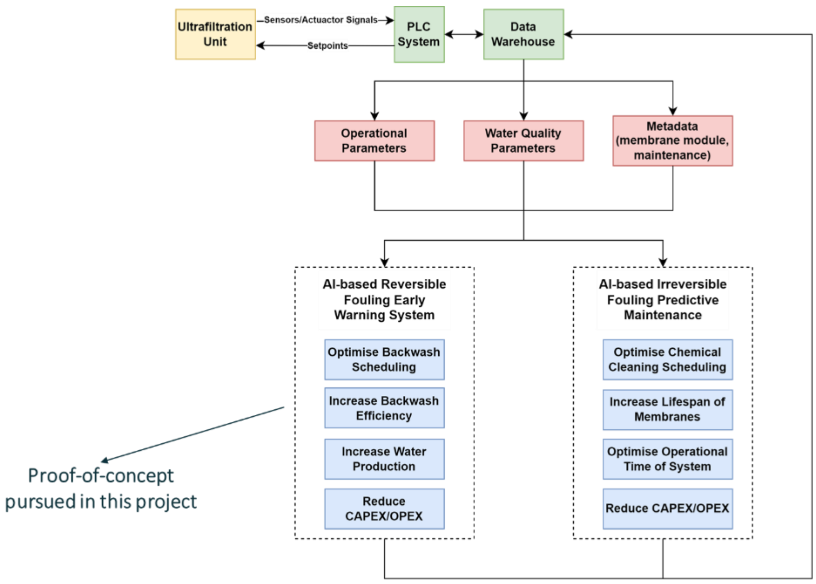

Early-Warning System and Predictive Maintenance Framework Envisaged for UF Membrane System Operations. Indication of Proof of concept pursued in this project and Outlook of the Future Work and Utilization of AI Forecasting Models in UF Installation Systems.

Interest: Predict the performance of membrane processes
With the innovation and development of technologies more attention has been paid to system efficiency, long-term performance prediction, and the integration of AI strategies into system operation. AI offers the learning ability, and the capability to deal with imprecise and highly complex non-linear data. AI can predict membrane fouling through learning mechanisms based on datasets rather than using mathematical equations.

Method: AI data-driven methods, experimental work at lab and full-scale monitoring
Our approach utilizes artificial intelligence (AI) with data-driven methods, employing neural network models trained on full-scale data. These models are developed using historical water quality and plant operations data, with a focus on predictive performance. After identifying optimal models for short-term transmembrane pressure (TMP) forecasting, their ability for recursive forecasts over an extended horizon is assessed. Through extensive data preprocessing and feature engineering, including a semi-automated method for TMP cycle and backwash event identification, AI models are trained. The primary objective is to understand underlying processes and predict TMP values for future filtration cycles. These models are tested across diverse water sources to evaluate their ability to generalize learning of membrane fouling and provide accurate predictions for various ultrafiltration systems.

Results: AI models trained to forecast the rise in TMP over subsequent filtration cycles
Neural network models were trained to forecast the initial and final TMP values up to 3 filtration cycles (where 1 filtration cycle is 18 minutes + 35 sec backwash) ahead using water quality and operational parameters as input, resulting in highly accurate predictions with R2 values exceeding 0.95. These results suggest that the employed data pre-processing and neural network modeling approach holds promise for forecasting the rise in TMP over subsequent filtration cycles, serving as an effective early warning system for the Heemskerk UF installation. To assess the model's generalization capabilities to other UF systems, preliminary tests were conducted using datasets from a different system – a UF pilot treating water from lake Valkenburg, operated by Dunea. Unfortunately, the models exhibited significantly poor performance when forecasting 1 filtration cycle ahead. The study also explored correlations between water quality parameters and membrane resistance in mini ultrafiltration tests, finding significant variations based on water type/location. Identified parameters for a potential early warning system include Biopolymers, MFI 45, SAC, Mn, MFI_UF, and turbidity, with SAC and MFI-UF showing strong correlation to non-backwashable resistance. SAC is recommended for full-scale monitoring. The study employs machine learning, utilizing SAC data to predict transmembrane pressure at a full-scale UF plant (Heemskerk). The data-driven model highlights SAC's significance in explaining and forecasting full-scale UF membrane fouling, suggesting its potential for improved modeling.

Implementation: UF installation forecasting optimizes operations, enhancing efficiency through backwashing, cleaning, and chemical consumption optimization in the future
The study's results offer valuable insights into the potential of AI-based methodologies for training data-driven models as an early warning system to anticipate membrane fouling in UF systems. The methodologies investigated can be further advanced and utilized to provide advanced operational guidance by optimizing backwashing intervals and cleaning intervals, along with the associated optimal chemical consumption but also significantly contribute to the security of supply in UF membrane installations. This contributes to a more robust water purification system for the project partners, with the potential for application and training in other UF installations in the future. The project's results and insights provide targeted recommendations for further data collection, suggestions for additional model training, and develop hybrid models that can stimulate the deployment of the early warning system into full-scale systems.

Report
This research is reported in report *AI-based reversible membrane fouling early warning system for Ultrafiltration* (BTO-2024.009).

Contents

1 Introduction

1.1 Project Background

Fouling of UF plants is largely dependent on the incoming water quality either inorganic (Fe, Mn), organic (natural organic matter, biopolymers) and/or biological (bacteria/virusses). Additionally, to the incoming water quality, membrane module characteristics and membrane operation also influence fouling. Despite pre-treatment, filterability can vary significantly throughout the year for surface water. In particular, the amount and types of organic/inorganic components and particles can vary and cause - without warning - operational problems. At PWN, in the summer of 2018, observed transmembrane pressures rise significantly quickly, leading to production capacity problems. To avoid such undesirable situations in the future, PWN is looking to understand the causes for membrane fouling and continuous monitoring on the operational parameters of the current installations and water quality parameters of the available surface water sources. Evides and Dunea are investigating the possibilities for full-scale application of UF at future treatment sites, which will be also fed with surface water.
If, in the future, changes in the water quality composition or operational strategies resulting in fouling of a UF installation could be noticed at an early stage, this would offer possibilities to take measures such as decrease back production, adjusting membrane backwash and cleaning intervals, adjusting chemical dosages and, if available, changing the source (in the case of PWN: Lek Canal water or IJsselmeer water), or in the long-term run adding additional pre-treatment. Furthermore, these insights offer (further) optimization of UF pretreatment, selection of the type of UF membrane elements, selection of cleaning chemicals and more efficient operation, e.g., backwash and cleaning strategies in a cost effective way.

1.2 Water Quality parameters: Influence on membrane fouling

This project follows the BO Research Project (402045/222) “Seasonal Effects of surface water on UF fouling potential”. In that project, water quality parameters were correlated with observed membrane fouling potential (based on derived parameters from operation such as trans membrane pressure (TMP) or membrane resistance build up) on ultrafiltration membranes (mini UF tests) where measurement series were conducted during the four seasons with dry weather (September 2020, December 2020, March 2021 and June 2021). The samples were taken from three Dutch locations, namely, Andijk (lake Ijssel raw), Heemskerk (lake Ijssel after pre-treatment) and Valkenburg (lake Valkenburg raw). The results of this project are summarized in section 4.1, and are used to provide insights on the decisions made and applied at the case study at Heemskerk.

1.3 Case study: Ultrafiltration Water Treatment Plant at Heemskerk

At the location Andijk from PWN, 100% of the raw surface water from Lake Ijssel is treated by drum screens, coagulation, flocculation, sedimentation, rapid sand filtration, and, approximately 20% of the total stream is consecutively treated by activated carbon after which it is transported in a 56 km long pipeline to Heemskerk (residence time pipeline ≈ 3 days). At Heemskerk, with a capacity of the water is treated by Ultrafiltration membranes with a total of 8 skids. This is one of the largest dual membrane facilities in the world, capable of treating 18 million m3 per year of pretreated surface water. It consists of two high performance membrane filtration steps, UF followed by RO.

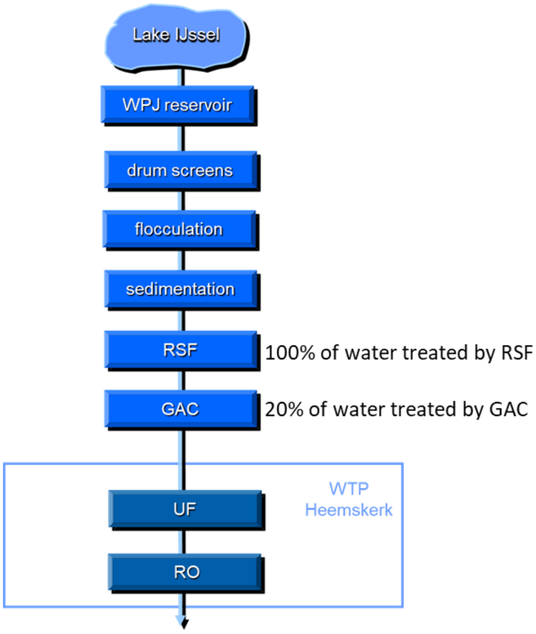

The dual-membrane system at Heemskerk comprises hollow fiber ultrafiltration modules followed by spiral-wound thin film composite polyamide reverse osmosis membranes. Both membrane filtration systems apply similar housing, UF is 1,5 m long with 200 mm wide, 4 elements per pressure vessel; while RO is 1,02 m long, 203 mm wide, 7 elements per pressure vessels, supported horizontally.
Membrane blocks are sited in two staggered rows separated by a wide central gallery. This layout was preferred since it provides sufficient space for straightforward pressure vessel replacement and also gives comfortable maintenance access. This solution also ensures a clear relationship of pumps with the treatment train.

Each UF membrane train is provided with a dedicated feed pump, rather than common feed pumps connected to a manifold. Main advantages of dedicated pumping are:

- Independent control of each membrane train
- Simplicity of installation and operation
- Avoids inevitable energy losses if feed flow is regulated to each block
- Higher overall pumping efficiency because of smaller range for the operating point.

The UF block comprises two symmetrical sets of 12 pressure vessels, each set being considered as a rack. The block has a single feed system that bifurcates into each rack. The racks also share a common filtrate manifold. The selected ultrafiltration membranes installed at Heemskerk are X-Flow elements with 0.8-mm-diameter hollow fibers. The feed flow enters from within the element's hollow fiber with permeate passing through the hollow fiber walls (inside-out flow).

1.4 Aim of the project

In this project, a proof of concept of an early warning system is proposed to predict fouling behavior (transmembrane pressure development) in full-scale UF membrane plants. In practice, the effects of fouling are translated into the applied flux. When membranes are operated with a constant flux, i.e. as a setting defined by the operator, the effects

of fouling are measurable by the development of TMP per time, independently from the type of fouling or fouling mechanisms being considered.
The ultimate goal for the water companies is to develop a forecasting tool that will be able to predict the fouling potential based on operational historical data obtained and support from water quality online monitoring. An AI-based data-driven approach is therefore adopted where neural network models are trained using the available full-scale data. Data-driven models are trained using historical water quality and plant operations data. Different model structures are evaluated based on their predictive performance. Optimal models are initially identified to predict TMP in the short-term and were subsequently evaluated on their capabilities of recursively providing forecasts over a horizon. The objective is to understand the underlying processes and generate predictions for TMP values associated with future filtration cycles. These models are also tested on datasets from another water source to assess their ability to generalize learning of membrane fouling behaviour and their capacity to provide accurate predictions for different ultrafiltration installation systems.
The results and insights of this project will provide recommendations that can be considered for further data collection, more advanced model trainings and the deployment of an early warning system into the full-scale system along with the UF plant management to prevent fouling of the practice installation.

2 Ultrafiltration membrane fouling and Artificial intelligence (AI)/Machine Learning (ML) models: brief overview

2.1 Ultrafiltration membrane fouling fundamentals

2.1.1 Factors affecting fouling

A major impediment to the improved performance of membrane separation processes, in general, is membrane fouling. The membrane is prone to chemical or biological deposition of matter. Membrane fouling occurs when undesired organic and inorganic substances accumulate on the surface of a membrane, obstructing/plugging pores and diminishing filtration efficiency hindering the permeate flow and compromising overall system performance. It results from complex interactions between the various foulants in the feed and the membrane surface (Cui et al. 2021).

Fouling can be described through several mechanisms, with designations varying per author. Mulder (1999) refers to concentration polarization, adsorption, gel layer and pore plugging, as fouling mechanisms; while flux decline, directly related with fouling mechanisms effects, is represented as resistance-in-series model where the resistance of a cake layer is in series with the resistance of the membrane itself. Other authors, consider cake layer formation as the main fouling mechanism in UF membranes (Wu et al. 2021). Independently from the fouling mechanisms considered, in practice fouling is translated into flux behaviour, meaning flux decline or flux increase. Overall, membrane fouling in UF can be divided into inorganic, organic and/or biological fouling, with mechanisms such as cake-layer formation, pore blocking/narrowing, adsorption of material onto the membrane surface, chemical interaction between solutes and membrane material, and bacterial growth (Goosen et al., 2005). However, when referring to the membrane pores, namely, there are four types of fouling: complete pore blocking, partial pore blocking, internal pore blocking, and cake layer formation (see Figure 1).
Fouling mechanisms are a product of the complex physical and chemical interactions between various feed constituents and the membrane surface (Nthunya et al. 2022). The major contributing factors to membrane fouling include (Al-Juboori and Yusaf 2012):

- Feed chemistry and composition, i.e., pH, ionic strength, and foulant concentration.
- Concentration polarization (CP): CP can be broadly described as the deposition of rejected solutes on the membrane's surface, creating a region near the membrane with spatially varying concentrations known as the polarized layer. This added resistance causes an increase in the osmotic pressure across the membrane, which decreases the driving force of the process (transmembrane pressure (TMP)), the permeate flux and the observed solute rejection, all of which increase the possibility of membrane fouling.
- Membrane properties include membrane material type, porosity, hydrophobicity, surface charges, membrane morphology, and molecular weight cut-off (MWCO).
- Process operating conditions such as temperature, pressure, aeration, permeate flux, and other hydrodynamic conditions.

Fouling has detrimental effects on the membrane's performance and integrity, as the deposition and accumulation of foulants on its surface and/or within its pores leads to a decline in the permeability (derived from flux and TMP), pressure drop and deterioration of selectivity, as well as a significantly reduced lifespan. These are normally the key performance indicators of membrane installations and fouling impacts all of them, likely with a decrease of permeability/flux, increase pressure drop and changes in selectivity (can be increase/decrease, usually decrease).

Different measures to mitigate fouling are normally increased, such as backwash, forward flush, enhanced backwash, air scouring, clean in place (chemical cleaning). Due the implementation of these measures, more energy and chemicals are used and add up to the operational costs. Intensive mitigation actions may cause membrane breaks which lead to reduced lifespan.

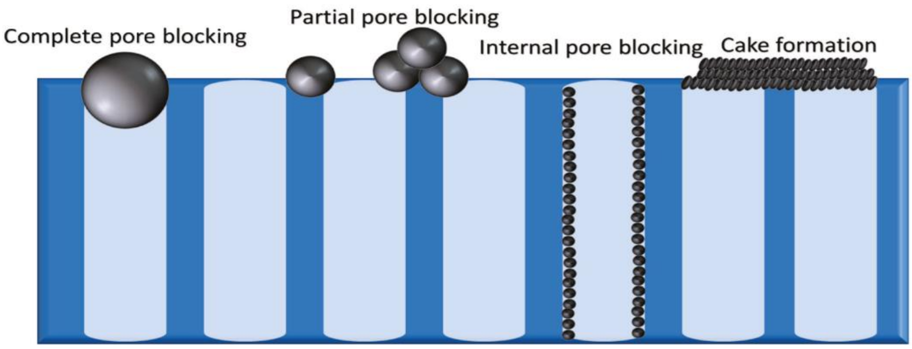

Figure 1 Types of fouling referring to membrane pores (AlSawaftah et al. 2022)

The topic of membrane fouling has been investigated intensely in literature, with multiple reviews having been written on the topic. Some of these reviews are focused on the general aspects of membrane fouling. For example, Guo et al. (2012) identified the major foulants which are particulate (inorganic or organic particles/colloids), organic (dissolved components and colloids e.g. humic and fulvic acids, hydrophilic and hydrophobic materials and proteins), inorganic (dissolved components e.g. iron, manganese and silica) and biological (algae and bacteria). Rudolph et al. (2019) presented a review of the state-of-the-art techniques used for in situ membrane monitoring. They showed that the majority of techniques offer monitoring of fouling layer thickness and distribution. However, it is now possible to investigate fouling layer thickness, distribution, composition, concentration and structural properties in high resolution and sensitivity. Moreover, various methods have been applied on many different experimental scales and types of membrane module. However, no single technique can provide all the information necessary to completely monitor all the interesting properties of the fouling development over time (Rudolph et al. 2019) . In other reviews, membrane fouling was examined in relation to a particular membrane separation method; for instance, Shi et al. (2021) reviewed the different techniques available for predicting fouling in membrane bioreactors. Their overview indicated that due to the complexity of membrane fouling, the predicting methods remain quite limited, and many assumptions are necessary to simplify them in order to make them feasible for calculations. Artificial neural network (ANN) was first applied to the predictions of factors related to membrane fouling due to its good modeling capability, and indeed achieved satisfactory results in a very short time. It has also been used to establish an input-output prediction model based on practical membrane fouling data. However, since membrane fouling mechanisms are complex and it is difficult to collect data, the establishment of an ANN-based membrane fouling prediction model still faces many challenges.

With respect to artificial intelligence (AI), Bagheri et al. (2019) and Viet and Jang (2021), presented cases of the application of AI to membrane fouling prediction. The comparison between the results of single models and hybrid models carried out by Bagheri et al. (2019) indicated that both approaches have high performance for the prediction of membrane fouling. However, the hybrid models achieve to intended results faster and do not need high expertise to tune the weights and functions of the modeling algorithms. Optimization algorithms are other intelligent techniques highly advantageous for optimizing the effective parameters related to membrane fouling. Viet and Jang (2021) systematically investigated the application of artificial neural network (ANN) models in predicting the system performance concluding that the developed models proved highly capable, with observed R2 values >0.9 and high level of accuracy. Moreover, appropriate input datasets are recommended for each simulation. The successful models developed point to the future potential of applying artificial intelligence-based techniques in the early prediction of the performance of membrane filtration processes.

2.2 Ultrafiltration in drinking water treatment

Driven by increasing drinking water demands in the Netherlands (+30% by 2040) (Vewin 2019), Dutch water companies are expanding their drinking water sources and/or exploring alternative sources. Open surface waters are considered a suitable candidate for a stable supply of significant volumes of water matching this future demand. Driven by more stringent drinking water quality requirements, current water treatment infrastructure ageing and climate change induced trends like salinization. Dutch drinking water companies are actively exploring or already applying ultrafiltration membrane technology for surface water treatment to either replace conventional pre-treatment or act as pre-treatment step for reverse osmosis (RO) membrane application (e.g., UF-RO plant Heemskerk, where UF is before RO) . Since surface water quality is particularly prone to seasonal variations, adequate and robust pre-treatment is required. Conventional surface water pre-treatment generally includes coagulation, flocculation, sedimentation and/or flotation, and/or (multiple) media filtration step(s). Compared to these technologies, the application of membrane technology in drinking water treatment offers many advantages, such as full retention of suspended solids, less complex operation and footprint (Kimura et al. 2004). Ultrafiltration (UF) membranes are especially attractive because they provide very high efficient removal (when integrity is uncompromised) of suspended particles and colloids, turbidity, algae, bacteria, parasites, viruses and large molecular weight organic matter for clarification and disinfection purposes at relatively low operating pressures (Van Der Bruggen et al. 2003). Looking at permeate water quality, conventional treatment steps can be replaced (Van Der Bruggen et al. 2003) and be outperformed by a single ultrafiltration membrane filtration step (Brehant et al. 2002).
Analysis of surface water quality variations and fouling potential assessment in various seasons can greatly aid the design stage and operation of such membrane systems (see section 3.1), especially when the source it surface water.

2.2.1 Ultrafiltration fouling on surface water matrix

Interactions between the membrane material and various compounds in the raw water can cause membrane fouling (Yuan and Zydney 2000) . In general, the smoother and the more hydrophilic a membrane surface is, the more resistant it is to fouling (Van Der Bruggen et al. 2003). Moreover, charged components tend to cause fouling because of electrostatic attraction between charged components and the charge-bearing membrane.
Various studies on surface, lake, and river waters have identified naturally occurring organic matter (NOM) as one of the major foulants during ultrafiltration treatment (Jermann 2008, Kimura et al. 2004, Yuan and Zydney 2000). Using liquid chromatography organic carbon detection (LC-OCD) analysis technique, NOM can be separated in distinct fractions. The general belief is that the fraction of humic substances are mainly responsible for irreversible fouling development on the membrane (Jermann 2008), but opposing observations have been documented (Tian et al. 2013). The correlation between the NOM fraction of biopolymers and UF membrane fouling has been validated as independent seasonal surface water quality variability (Tian et al. 2013). Polysaccharides, an example of the NOM biopolymer fraction, causes both irreversible and reversible fouling by pore blocking and cake/gel formation (Jermann 2008). Particulate matter (characterized by suspended solids and turbidity) are also found to correlate well with UF membrane fouling (Chew et al. 2017, Tian et al. 2013). Algal organic matter (AOM), consisting mainly of biopolymers (polysaccharides and proteins) and low molecular weight organic compounds (humic-like substances) and released during algal blooms show high correlation with UF membrane fouling by pore blocking and compressed cake filtration fouling mechanisms (Villacorte et al. 2015). Presence of calcium seem to enhance interactions between foulants and the membrane (Jermann 2008).

2.3 Modelling and prediction of fouling

Efficient prediction techniques and diagnostics are integral for strategizing control, management, and mitigation interventions to minimize the damage of fouling occurrences in the membranes.
Membrane fouling is an inevitable aspect of membrane operations; however, real-time, fast, and accurate predictions of membrane fouling can enhance its membrane (plant) control, improve the efficiency of membrane operations as well as drastically reduce the involved operating costs (Koo et al. 2013, Shi et al. 2021). The techniques used to predict membrane fouling have been reviewed (AlSawaftah et al. 2021). Briefly, fouling prediction techniques include pilot plant evaluations of the system's performance, the use of fouling indices, and the use of predictive mathematical models. Pilot plant studies involve the design of an optimal system based on the characteristics of the feed. Information obtained from the analysis of the proposed water source is used to develop a pretreatment scheme for the feed water, evaluate the compatibility of one or more types of membranes with the feed water, as well as determine the optimal operating conditions. Pilot plant tests are run for long hours (several thousand hours) to gauge the performance of the membrane system. Although this method generally provides reasonably good predictability of membrane fouling, it is extremely costly and time-consuming. Membrane fouling indices are predictive quantifiers that indicate how susceptible membranes are to fouling. The traditional and most widely applied fouling indices are the silt density index (SDI), the modified fouling index (MFI), Langelier Saturation Index (LSI) and Stiff and Davis Saturation Index (S&DSI); however, these indices have several limitations, and current research efforts have been devoted to improving the reliability and accuracy of these indices in predicting fouling-propensity (AlSawaftah et al. 2021). Fouling prediction models are valuable because they facilitate the optimization of fouling removal and prevention methods, and also help establish interactions and relationships between different filtration variables. Mechanisms such as pore-blocking and cake formation are mathematically represented in equations. Some of the mathematical models developed to describe membrane fouling are listed in Table 1. Recently, the use of AI in predicting membrane fouling, e.g. in ultrafiltration (see Annex I Table AI.1), has gained attention due to its adaptive capability and prediction accuracy (Bagheri et al. 2019, Niu et al. 2022).

Table 1 Conventional membrane fouling models

Fouling model	Description
Resistance-in-series (RIS)	-Enable the determination of the fouling resistance form -Vary with fouling mechanism(internal/external)
Pore blockage/Hermia's models	- Describe the filtrate flux under constant pressure - Four blocking modes: complete pore blocking, standard blocking or pore constriction, intermediate poreblocking, and cake filtration
Combined cake filtration-pore blockage models	- Assume that the fouling occurs in three stages: pore constriction, pore blocking and cake accumulation

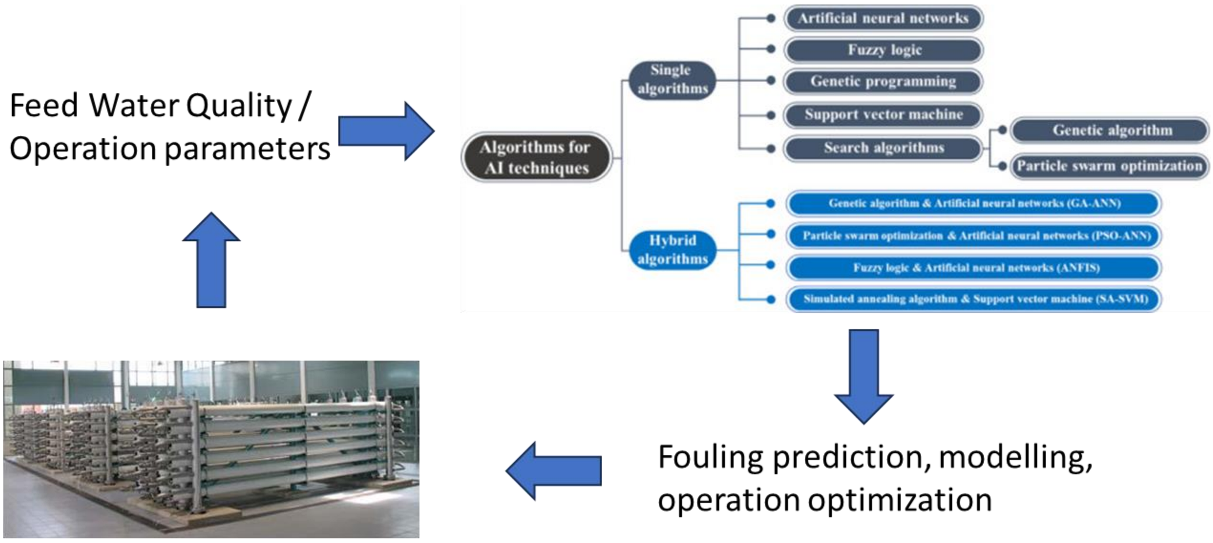

Figure 2 Approach of use of artificial intelligence (AI) in membrane fouling prediction.

Figure 2 shows the commonly used algorithms for AI techniques in prediction of membrane fouling. They need input data that can be from operational parameters or water quality (mainly online data generated), and will produce as an output a prediction, calculation, model, or optimized models. Generally, algorithms for AI techniques mainly include artificial neural networks (ANN), fuzzy logic (FL), support vector machines (SVM), genetic programming (GP) and search algorithms. Search algorithms including genetic algorithms (GA) and particle swarm optimization (PSO) are important optimization approaches. Search algorithms can be used to optimize the performance of modeling techniques to jointly guide the optimization of operating conditions in membrane separation processes. Besides, these search algorithms can be coupled with other modeling algorithms, such as ANN, FL and SVM (Niu et al. 2022).

2.3.1 AI Data driven/Machine learning: Artificial neural networks and deep learning

AI is an interdisciplinary field in which machines mimic human cognitive functions such as learning, problem-solving, reasoning, and perception. In simpler terms, AI can be defined as intelligence exhibited by machines whose techniques use historical data to learn about the system and adapt its decision-making processes (Alam et al. 2022).

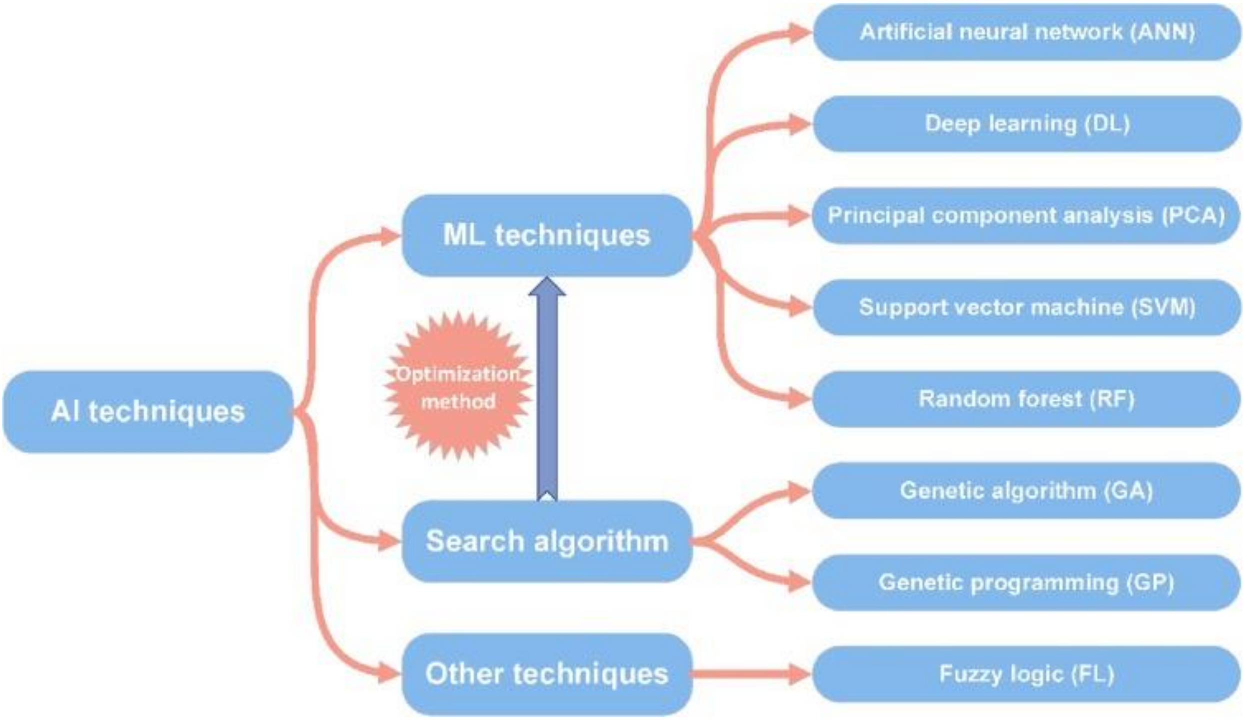

Figure 3 Classification of AI and ML techniques used in drinking water treatment (Li et al. 2021).

Figure 3 shows the AI and ML technologies commonly used in drinking water treatment. Machine Learning(ML) is commonly used to solve four types of problems: classification, regression, dimensionality reduction and clustering. ML methods used to solve regression and classification problems build predictive models based on process data. A complete ML method application process includes the following: i) estimating the relationship between the input parameters in the system and the target output from a given data set that is, the training process and ii) using the estimated nonlinear relationship to predict the new output of the system (Li et al. 2021). The goal of ML is to predict rather than estimate, and that is why it is important for fouling forescasting.

From the different ML techniques (see Figure 3), for example, artificial neural networks (ANN) , deep learning (DL), support vector machine(SVM) and random forest (RF) are used to handle nonlinear classification and regression analysis (Li et al. 2021). ANN and DL both imitate the behavioural characteristics of animal neural networks and perform distributed parallel information processing the difference between them is that DL has a more complex structure and usually has higher prediction accuracy than ANN. However, DL relies on a larger amount of data to train the network and is more prone to overfitting (Schmidhuber 2015). In contrast to the classic ANN, the SVM has stronger mathematical theory support, which enhances the interpretability of the model to a certain extent. However, SVM models are difficult to train based on large-scale sample data and requires a long training time (Li et al. 2021). Compared with ANN, DL, and SVM, a significant advantage of RF is that it can evaluate the importance of variables while completing classification or regression analysis. Principal component analysis (PCA) has been used as a dimensionality reduction method is mainly used to process high-dimensional data (i.e., fluorescence excitation-emission matrix (EEM). Search algorithms are a method of finding the optimal solution of multiple solution problems under certain constraints. The commonly used search algorithms in DWT are genetic algorithm (GA) and genetic programming (GP). They are both global optimization methods that simulate the biological evolutionary process in nature, and the main difference between them is the depiction of the programme or algorithm(Li et al. 2021). Fuzzy logic (FL), a method based on multi-valued logic, uses fuzzy sets to study fuzzy judgement, which allows FL-based fuzzy inference systems to simulate the human brain to implement natural inference.

AI algorithms such as artificial neural networks (ANN, fuzzy logic (FL), and support vector machine (SVM) among others have been applied to predict membrane fouling (Table 2) (Bagheri et al. 2019, Niu et al. 2022, Xu et al. 2021).

Due to the ability of robust autonomous learning, many researchers have used ANN to deal with environmental problems by solving multivariate non-linear problems (Viet et al. 2022). Currently, ANN is the mainstream AI algorithm because of its ease of implementation and relatively high accuracy. ANN has a powerful information storage and computational capability by using "black-box" learning methods. It has been increasingly studied in UF membrane systems.

Despite the potential of AI in predicting membrane fouling, some concerns have been raised regarding the use of these non-mechanistic modeling tools to correlate operating variables with performance parameters. The main concern is that these models are not based on physical or chemical phenomena and rely on calibrations 'learning' using experimental data. If there are any sudden changes in operating parameters, the models may be susceptible to overfitting, and misleading correlations. Their "black box" nature does not provide information about the physical phenomena involved. The selection of the proper modeling tool is also very important for the predictive accuracy. These issues can be overcome by simplifying model structure, optimizing input parameters, ensuring that the data sets used in the learning stage are large enough, and performing cross-calibrations across the entire calibration data set to optimize the internal structure of the algorithm and minimize data overfitting. On the other hand, the knowledge about the contribution and impact of each input in predicting outputs from the model provides mechanistic insight into the modelled processes. The use of hybrid (mechanistic and non-mechanistic) models and combining several AI models has been proposed to improve prediction accuracy and overcome the weaknesses of a single AI model (Galinha and Crespo 2021, Li et al. 2021, Niu et al. 2022).

The predictive models presented provide promising results, however, they are limited to predicting TMP based on data at a present point in time. Implementing models to forecast TMP could provide better decision-support for operators to adjust for membrane fouling before it occurs (Kovacs et al. 2022).

Table 2 Summary of artificial intelligence (AI) techniques commonly used in membrane fouling prediction (adapted from (Alam et al. 2022, Niu et al. 2022, Zhao et al. 2020)

AI Technique	Mode of Operation	Applications	Advantages	Disadvantages
k-NN	-Saves all existing data -Classification of new data points based on similarity	-Regression -Classification	-Easy implementation	- Computationally expensive - Memory intensive - Overfitting
DT	-Generates a training model to teach simple decision rules	-Regression -Classification	-High accuracy -Easy implementation -Applies to continuous and discrete data	-Instability -Overfitting
RF	-Creates DTs on data samples -Makes predictions based on each DT -Uses a voting mechanism to select an optimal solution	-Regression -Classification	-Decreased overfitting -Suitable for large datasets	-Not suitable for imbalanced datasets -Low training speed
A N N	-Statistical models built based on human brain neurons	-Pattern recognition -Performs nonlinear computations	-Fast prediction -Good for arbitrary function approximation -Suitable for high-dimensional datasets	-Computationally expensive -Difficulty in interpreting trained models
FNN	-Combines fuzzy logic and NNs	-Pattern recognition -Density estimation -Regression -Classification	-Can be used when a mathematical model does not exist for a problem -Easy implementation and interpretation	-Theoretical knowledge necessary -Computationally expensive

CNN, FFNN	-Uses convolution instead of matrix multiplication	- Image/video recognition - Classification - Regression - Segmentation	- Accurate results - Good speed	-Computationally expensive -Complex architecture
DNN	Input, output layers - Includes hidden layers	-Learning complex models -High-dimensional data processes	-Best performance if enough data are available -Suitable for nonlinear data -Fast prediction following training	-Computationally expensive -Requires more training data
SVM	-Requires labeled training data for each category to identify the next step -Mapping input vector into a high -dimensional feature space	-Classification -Regression -Pattern recognition	-Suitable for high-dimensional datasets -Suitable for linear and nonlinear datasets	-Computationally expensive -Difficult to train -Overfitting -Not suitable for noisy data
GA	-Produces the optimal strategy to solve complicated problems under a particular theory	-Regression -Clustering -Classification	-Provides multiple solutions -Supports multi -objective optimization -Suitable for discrete and continuous data	-Difficult to implement -Computationally expensive -Time-consuming
PSO	Optimizes a problem by iteratively improving a candidate solution with regard to a given measure of quality	-Clustering -Regression -Classification	-Easy implementation -Parallel computation	-Mathematical background needed for evaluations -Difficult to define initial design parameters

Abbreviations: k-NN, k-nearest neighbor; DT, Decision tree; RF, Random Forest; ANN, Artificial neural networks; FNN, Fuzzy neural networks; CNN/FFNN, Convoluted/feed-forward neural networks; DNN, Deep neural networks; SVM, Support vector machine; GA, Genetic algorithm; PSO, Particle swarm optimization.

2.3.2 Membrane fouling development

Piron et al. (1997) used ANNs to assist in crossflow microfiltration, and two different modelling methods were proposed. One did not require an accurate description of the process and relied on only the learning capabilities of ANNs to approximate the dynamics of the microfiltration system. The other was a semi-physical model that established a prediction model by combining prior knowledge, and the neural network was used only to evaluate unknown parameters. The prediction of the semi-physical model was precise, probably because part of the phenomenon was explained by the integration of the mass balance equation.
Chew et al. (2017) combined Darcy's law on cake filtration and an ANN into a semi-physical model to predict dead-end ultrafiltration. The formula parameters that initially needed to be experimentally determined were predicted by ANN, which provided a reliable method for predicting the fouling propensity of the UF membrane achieving good predictions.
Krippl et al. (2020) used ANN to predict the ultrafiltration flux and the prediction result worked as a parameter of the differential equation, forming a combined model for the duration of crossflow ultrafiltration. It has good adaptation to varying filtration characteristics (RMSE < 6.2) compared to a mechanistic membrane model and can use the same training set to process batches and feed batches for ultrafiltration. The interpretation of this model might be more accessible than simply using ANN because it is based on physical mechanisms.

Teodosiu et al. (2000) trained a ANN to describe the flux evolution during the hollow fibre membrane ultrafiltration process and to predict the flux of the entire process from ultrafiltration to backwash. The trained networks are able to accurately capture the non-linear dynamics for initial fluxes in the range 80–145 l h^{-1} m^{-2} and for time horizons up to 2500 s, offering a fairly accurate description of experimental flux evolution and, thus, creating theoretical premises for further approach to the optimization of the process.

Delgrange et al. (1998) developed a ANN to predict the evolution of transmembrane pressure (TMP) from some operating conditions and water quality parameters, for a pilot producing drinking water by ultrafiltration of natural water. This neural network model fits experimental data with a very good accuracy. Four inlets were sufficient to correctly predict TMP at the end of current filtration period and after next backwash, for this water resource into the given experimental domain. These parameters are turbidity, permeate flow rate, TMP at the filtration start and TMP before previous backwash.

Delgrange-Vincent et al. (2000) used back propagation artificial neural network (BPANN) to successively predict the transmembrane pressure (TMP) of pilot plant short-term and long-term ultrafiltration processes. The ANN made precise predictions for a long time, even in the case of water quality changes, which indicated that full AI models are suitable for application for control purposes.

Among other ML methods, DL, which has received particular attention in the past decade in the field of AI, can provide far higher performance than ordinary ANN (Zhao et al. 2019). For example, even though not applied for UF but for NF/RO, Park et al. (2019) used a convolutional neural network (CNN) to predict the increase in nanofiltration or reverse osmosis membrane fouling and the decline in flux via regression. The model was developed based on high-resolution dirt layer images. Compared to ANN, image prediction-based CNN with a DL framework does not need to define specific relationships between fouling parameters and shows high performance in extracting valuable functionalities from large amounts of data. The prediction performance is excellent (R2 value is 0.99), however, due to the large amount of data and the complexity of the network, the modelling period of CNN is long, and its applicability needs further research.

Viet and Jang (2021) systematically investigated the application of ANN models in predicting the system performance of osmotic membrane bioreactors (OMBRs). Even though, FO fouling is very different from UF fouling mechanisms, the successful models developed in this work point to the future potential of applying artificial intelligence-based techniques in the early prediction of the performance of membrane filtration processes. Liu and Kim (2008) compared the performance of mathematic and mechanical model (blocking laws) with ANN model for UF process. Compare with the blocking laws, ANN model achieved excellent agreement between prediction and experimental TMP values. In comparison with the classical pore-blocking models which need to be fitted for each experimental test, ANN is capable of simulating all the experimental data instantly. To provide an early warning of the membrane fouling, Chew et al. (2017) combined Darcy's law and ANN to predict the specific cake resistance and total suspended solids in a UF pilot plant by inputting the data of feed water turbidity, filtration time and TMP. This hybrid model could be easily implemented in the industrial-scale UF treatment plant as it did not need any additional costly analysis equipment. Curcio et al. (2006) and Corbatón-Báguena et al. (2016) used feed-forward networks to predict permeate flux decay which showed to be successful. Chen & Kim (2006), applied radial basis function (RBF) and BPANN models and compared them with multiple regression models. Results indicated that the RBF neural network outperformed the other methods and was able to predict permeate flux with a limited number of training points (O'Reilly et al. 2018).

Based on the developments from previous research and the type of operational and water quality data, and after discussing with the project partners, a good way forward is to employs an artificial intelligence (AI)-based data-driven methodology, utilizing neural network models trained on comprehensive full-scale data. These data-driven models leverage historical water quality and plant operations data, with a thorough evaluation of various model structures based on their predictive performance.

3 Materials and Methods

3.1 Screening of water quality parameters to predict fouling

3.1.1 Water sampling

From three locations in the Netherlands (Andijk (lake Ijssel raw), Heemskerk (lake Ijssel after pre-treatment : coagulation, flocculation, sedimentation, rapid sand filtration and (partial; 20%) activated carbon filtration) and Valkenburg (lake Valkenburg raw)), twenty litre samples were collected all on a single day with dry weather conditions in September 2020 - Autumn, December 2020 - Winter, March 2021 - Spring and June 2021- Summer. At Andijk, 100% of the raw surface water from Lake Ijssel is treated by rapid sand filtration, approximately 20% of the total stream is consecutively treated by activated carbon after which it is transported in a 56 km long pipeline to Heemskerk (residence time pipeline ≈ 3 days). Lake Ijssel samples were collected on-site from drinking water company PWN sampling points and lake Valkenburg samples were collected 20 cm below the water surface. Sample collection, dark transportation and analysis preparation was always performed on 1st day of the week. Samples were stored at 4°C.

3.1.2 Water quality analysis

All water quality parameters and water quality indicators measured except dry matter analysis (KWR lab), MFI0.45 (ASTM 2019) analysis (KWR lab) and MFI-UF analysis (IHE Delft) were either taken from the regular analysis programme of the corresponding drinking water company (lake IJssel samples) or analysed by the Aqualab Zuid and KWR lab (lake Valkenburg).

Acidified samples were analysed for Fe (Limit Of Detection LOD: 30 µg/L), Mn (LOD: 10 µg/L) and Ca (LOD: 0.5 mg/L) by inductively coupled plasma mass spectrometry (ICP-MS) using the Thermo Scientific iCAP RQ (Aqualab Zuid & HWL) and the Thermo Fisher Scientific XSERIES 2 (KWR). Total and dissolved organic carbon analysis was measured by non-dispersive infrared detection (NDIR) using a Shimadzu TOC-L$_{CPH}$ (HWL) and Shimadzu TOC-V$_{CPH}$ total organic carbon analyser (KWR) (LOD = 0.2 mg C/L). Bicarbonate was analysed using the Skalar Robot SP-2000 Metrohm Titrino 848 (HWL) and by a titrimetric method using hydrochloric acid (KWR) (LOD: 6.1 mg HCO_3/L). Dry matter analysis was performed thermogravimetrically by determining the weight of the non-volatile solids at 105°C (dry organic and inorganic matter), 550°C (inorganic matter) and 1025°C (calcite residue) (KWR) (LOD: 1 mg solids per sample-volume processed). Suspended matter analysis was performed gravimetrically on particles retained by glass-filter (HWL) and >0.45µm (KWR) (LOD: 1 mg/L). Liquid chromatography – organic carbon detection (LC-OCD) analysis of the surface water samples were performed after in-line 0.45µm filtration by chromatographic detection of organic carbon, UV absorbance (254 nm) and organic nitrogen. (DOC-Laboratory Dr Huber, following (Huber and Frimmel 1992)). During analysis, natural organic matter (NOM) present in the sample was fractionated into biopolymers (BP; >>1 kDa; polysaccharides, proteins, amino sugars), humic substances (HS; 0.5 – 1.2 kDa; humic- and fulvic acids), building blocks (BB; 0.3 – 0.5 kDa; hydrolysates of humic substances), low molecular weight acids (LMWA; <0.35kDa; aliphatic LMW organic acids) and low molecular weight neutrals (LMWN; <0.350 kDa; alcohols, aldehydes, ketones, sugars and amino acids)(Abushaban et al. 2022). The sum of these five fractions is called chromatographable DOC (CDOC). The hydrophobic organ carbon (HOC) is equal to the difference between DOC and CDOC. The spectral absorption coefficient (SAC) was measured for the HS normalised over the organic carbon value for HS and provides a measure of the degree of aromatic and unsaturated structures in the sample. Turbidity was measured using the Hach 2100HQ (LOD: 0.1 NTU). Electrical conductivity was measured using a Radiometer CDM 83 conductivity meter. Saturation index was calculated according to the standard method of HWL laboratory. The membrane fouling index using 0.45µm membrane filters (MFI-0.45µm), a measure of flux decline at constant pressure and was developed as an aid in predicting the rate of fouling of reverse osmosis membranes by a specific type of raw water (Schippers and

Verdouw 1980) was measured using a Con-vergence Inspector SDI/MFI meter equipped with 0.45µm SDI filters (type: AAA1013).
The application of ultrafiltration membranes instead of filters of 0.45µm pore size is referred to as MFI-UF (Boerlage et al. 2002). The modified fouling index with ultrafiltration (MFI-UF) membranes at constant flux filtration was used for measuring the particulate and colloidal fouling potential of the water samples. The protocol followed is described in (Salinas-Rodriguez 2011, Salinas-Rodriguez et al. 2015, Salinas-Rodríguez et al. 2021) where 10 kDa MWCO membranes made of polyether sulfone (PES) (Millipore, Ireland) were used. The testing flux during filtration was 100 L/m2/h. Samples were stored at 4 °C and tested within 3 days of the sampling date. The average membrane resistance of the membrane filters was 8.96×10^{11} 1/m ± 3.4×10^{10} 1/m (3.8 % coefficient of variation). Testing was performed in duplicates and reported the average value. The limit of detection of the method was reported as 50 s/L^2. MFI-UF values are per definition normalized to standard temperature, pressure, and filter area conditions.

3.1.3 Ultrafiltration membrane used

UF modules were constructed in-house. Hollow fibers extracted from a commercially available Pentair X-flow RX-300 0.83 UFC (former: UFC M5) hydrophilic PES/PVP ultrafiltration membrane module (product no: 300099081, article code: 1051BL395A) having a typical MWCO of 150-200 kDa (Kennedy et al. 2005) were operated in inside-out filtration mode during the fouling behaviour experiments. The hollow fibers have a typical pore size of 18 nm (Floris et al. 2016). Lab-scale membrane modules were prepared by potting membrane fibers with an epoxy resin in a transparent poly vinyl chloride tube of 19.5 cm length and 17 mm diameter, similar to the method previously described by Floris et al. (2016). With an effective hollow fibre length of 17 cm and a hydraulic diameter of 0.83 mm the resulting membrane filtration area was 8.9 cm^2.

3.1.4 Membrane fouling characterisation measurements

On the 2nd, 3th and 4th day of the week the UF fouling experiments were performed on raw lake Valkenburg , raw lake Ijssel and pre-treatment lake Ijssel water, respectively. 24 hours before the experiment, samples were taken from the 4°C storage. During experiments, sample temperature was kept constant at 20°C (± 1°C). An automated laboratory scale set-up was used for the ultrafiltration fouling behaviour experiments at constant flux, alternately running in filtration- and backwash mode (see Figure 4, designed by KWR (The Netherlands)). The feed water was continuously fed at a constant flow by a pulsation-free neMESYS piston pump (Cetoni GmbG, Germany). The temperature and transmembrane pressure (TMP) at atmospheric permeate outlet pressure were measured and logged by a pressure probe (WIKA CPG1500) every five seconds. Each experiment consisted of four phases: 1) membrane conditioning using ultrapure water, 2) single ultrapure water full filtration cycle to determine the clean membrane resistance, 3) six filtration cycles on surface water sample (duration: 18 minutes, flow:0.18 L/h, corresponding flux: 200 L/m^2.h) and six backwash cycles (0.23 L/h corresponding to 250 L/m^2.h, 30 seconds each) and 4) single ultrapure water full filtration cycle to determine fouled membrane resistance . A manual backwash was initiated in case pressure build-up exceeded 3.0 bars within the original 18 minute filtration cycle duration. Ultrapure water (Veolia Elga Purelab Chorus) was used for backwashing and the backwash flow was provided by a pressurised vessel (3 bars) combined with an adjustable flow control.

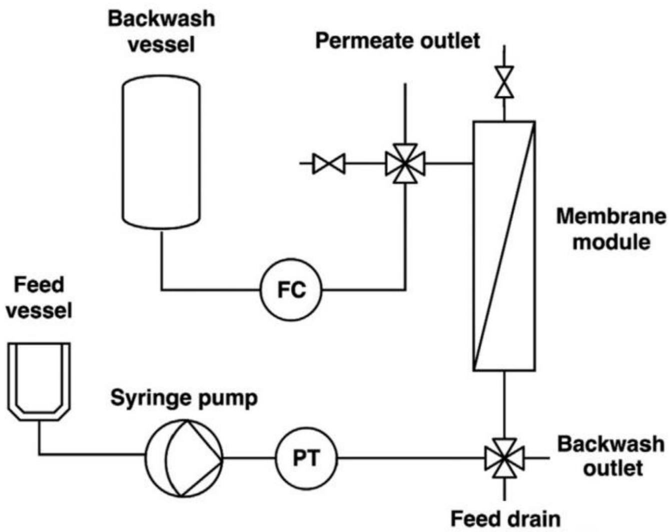

Figure 4 Schematic overview of automated membrane operation system used for the UF fouling experiments. During filtration cycle, water is transported from the feed vessel to the permeate outlet (dead end filtration, inside-out operation). During backwash cycle, ultrapure water is pushed through the membrane (outside-in operation) and collected in the backwash outlet. PT: pressure transmitter, FC: flow controller. Adapted from (Ahmad et al., 2020).

3.1.5 Membrane resistance calculations

The best-fit linear curve was calculated for each experiment from the pressure build-up in all six filtration cycles. Because of the automated valve action after each filtration-backwash cycle and the low flow of 0.18 L/h, the first few minutes of each full filtration cycle showed a non-linear pressure build-up pattern. In addition, few experiments reached a pressure >3.0 bars within 15 minutes already, forcing a manual backwash due to system safety limitations. For these reasons, the slope of the best linear fit of the data points of the last half (9 minutes) of each filtration cycle was determined. From the average pressure build-up over six filtration cycles and the difference between the clean and fouled membrane the reversible and the non-backwashable resistance to filtration were calculated (Floris et al. 2016), respectively, following the resistance in series fouling model approach described by (Di Bella and Di Trapani 2019) using temperature-corrected water viscosity (Reid et al. 1987).

3.1.6 Data and correlation analysis

Statistical correlation and significance analysis of between both endpoints (reversible and non-backwashable fouling resistance values) with water quality analysis data was performed using Pearson correlation in Python 3.9 with the packages pandas 1.2.1 and SciPy 1.5.2. A negative correlation means that the endpoint decrease with water quality parameter and a positive correlation the opposite. The closer the correlation coefficient is towards -1 or 1, the better the correlation. The significance analyses (p-value) shows the probability that the correlation coefficient was in fact zero. A correlation with a associating p-value lower than 0.05 is regarded as significant.

Principal component analysis (PCA) was performed in Python 3.9 with scikit-learn package 0.24.1. In a PCA, the dimensions are reduced by introducing principal components that are linear combinations of the endpoints and water quality parameters. In our study, two principal components were used. A PCA score plot shows the projection of the data on the two principal components. A PCA loading plot shows how each parameter influences the two principal components, and it also shows how parameters are correlated (small angle between parameters means highly correlated, 90 degrees angle means highly uncorrelated).

3.2 Online measurement of Water Quality parameter (SAC) to support AI modelling

Based on the screening of water quality parameters to predict fouling and the possibility to online data acquisition, an UVAS plus SC 50 mm (HACH) with flow though unit and digital controller SC4500 was installed at the header of the UF unit at Heemskerk (PWN) for monitoring the spectral absorption coefficient (SAC) of the pretreated water entering the full scale installation (Figure 5). The monitoring was carried out for a period of three months during the transition from winter to spring where changes in the water quality are expected.

Figure 5 SAC sensor (HACH) installed ad Heemskerk, PWN full-scale Ultrafiltration installation.

3.3 Data-driven Models for Forecasting TMP and Reversible Fouling

Reversible fouling is typically associated with the rise in TMP (or resistance) within a filtration cycle, that is addressed by conducting a backwash between cycles. The backwash leads to the reduction of TMP which is measured to be lower than the final TMP witnessed for the prior filtration cycle. However, over longer time periods, the reversible fouling dynamics influence the long-term irreversible fouling, which requires chemically enhanced backwashes to address such a challenge. Such dynamics is well illustrated in the Figure 6, provided below. It can be seen that the optimised operations of membranes in handling the reversible fouling in short-term dynamics through increased backwash efficiency and better insights on the fouling potential, can lead to better management of irreversible fouling to ensure security of drinking water supply and longevity of the membranes.

As a result, an early-warning system and predictive maintenance system has been envisaged to enable the efficient and full-proof operations of UF membrane system. This has been illustrated in the framework provided in Figure 7. Therefore, to support the development of the first steps of the AI-based reversible fouling early-warning systems to reduce the long-term effects of reversible fouling and optimise operations at shorter-time constants, various data-driven models and training approaches have been explored to forecast TMP (or the rise of it) and also assess the generalisation capabilities of these models. Furthermore, the importance of certain input parameters in making predictions have also been investigated.

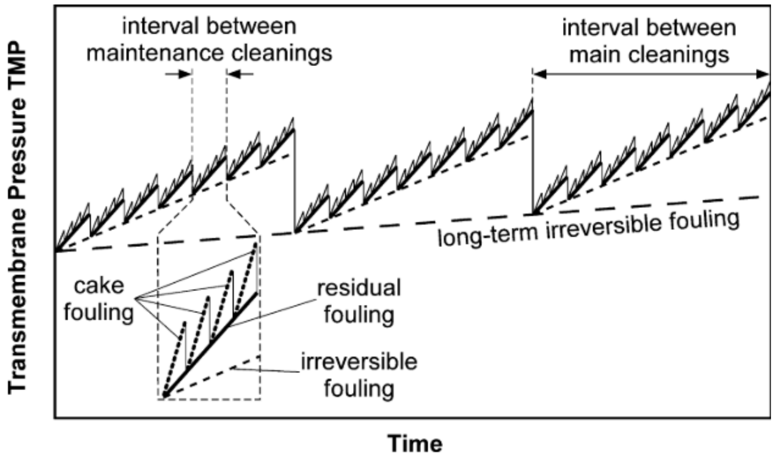

Figure 6 Reversible and Irreversible fouling dynamics as seen with short-term and long-term TMP increase (Kraume et al., 2009)

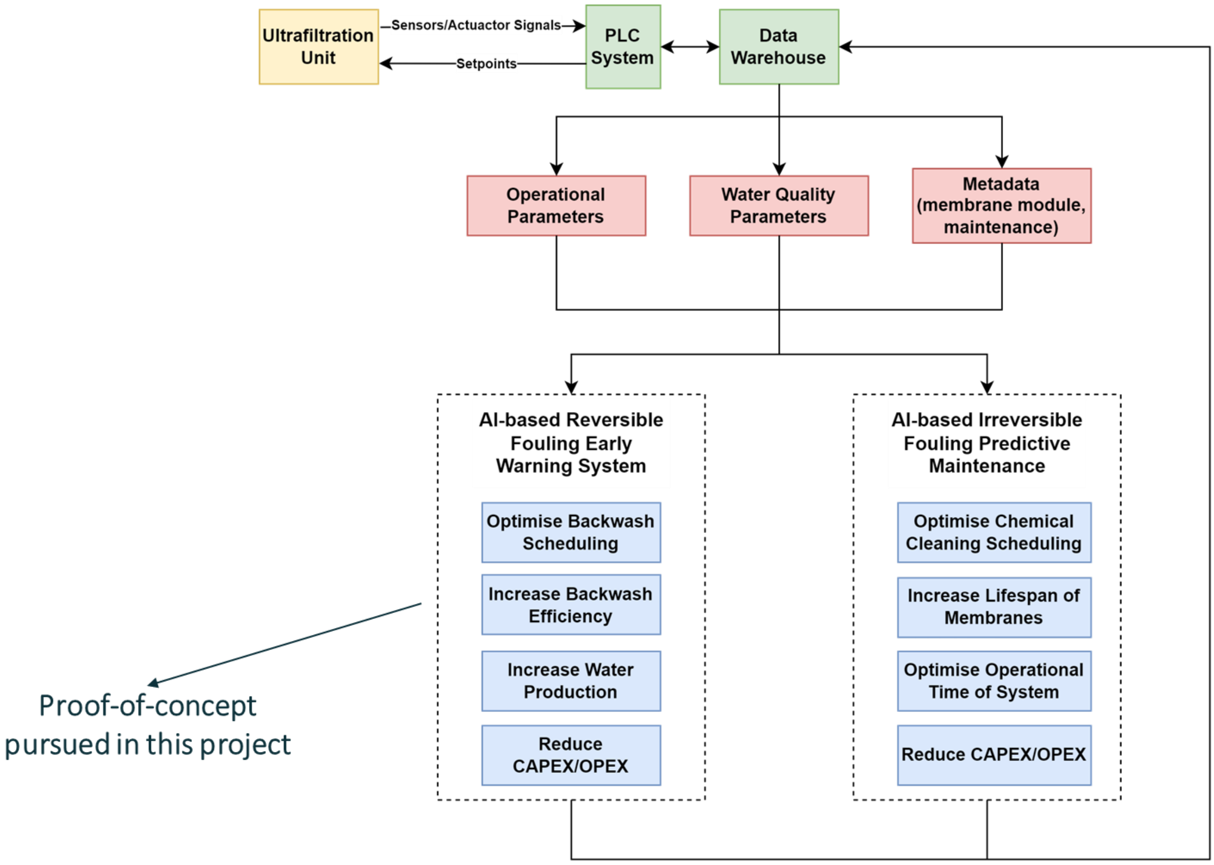

Figure 7 Early-Warning System and Predictive Maintenance Framework Envisaged for UF Membrane System Operations. Indication of Proof of concept pursued in this project and Outlook of the Future Work and Utilization of AI Forecasting Models in UF Installation Systems.

3.3.1 Data Overview

The training of machine learning and neural network models utilised various environmental and operational data. All data were based on online measurements. These variables included water quality and operational parameters: feedwater turbidity, feedwater temperature, feedwater flowrate and transmembrane pressure (TMP) for each membrane module. The total duration of data used for these variables amounted to 8 months. As described in Section 3.2, SAC data of a shorter duration of 3 months was also collected during this project and utilised. In Heemskerk (PWN), there are 8 parallel UF membrane modules in operation. Considering the diverse membrane performances observed during the initial data exploration, the membrane modules 7 and 8 were selected for the analysis and testing of methodologies. Furthermore, the measured granularity of the data varied, as provided in the overview in Table 3.

Table 3 Measured variables from Hermskerk Ultrafiltration installation (PWN) and the associated granularity available

Variables	Variable Type	Unit	Granularity
Feedwater turbidity	Water quality	FTU	15 mins
Feedwater temperature	Water quality	°C	15 mins
Feedwater flowrate	Operational	m^3/h	15 mins
TMP (module 7)	Operational	kPa	15 mins
			10 secs
TMP (module 8)	Operational	kPa	15 mins
			10 secs
SAC	Water quality	m^{-1}	1 min

Certain static information associated with the membrane characteristics and operations were known. The filtration cycles for all membrane modules was set to 18 minutes, with a backwash of approximately 25 seconds occurring in between. The backwash flowrate is set to 1000 m^3/h. The membrane surface area is 3840 m^2. In addition to the primary data from the PWN installation at Heemskerk that was utilised for model training and testing, a secondary dataset provided by the water company Dunea was also utilised. The dataset was from the UF pilot installation that treats the water from the lake Valkenburg amounting to 01/10/2022 – 16/10/2022. An example time period of the dataset has been provided in Figure 8.

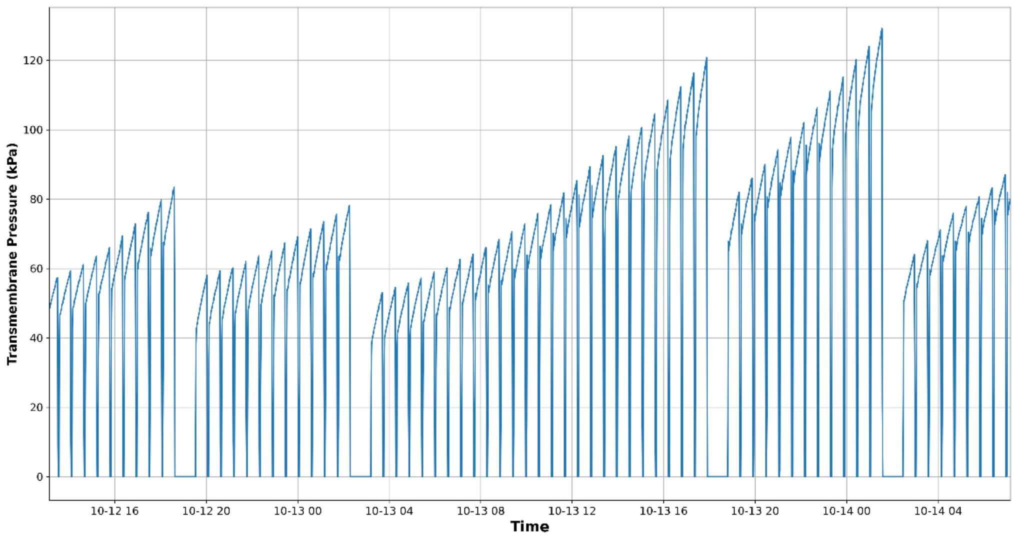

Figure 8 Raw Dataset of the Transmembrane Pressure recorded in the UF Pilot Installation Operated by the Water Company Dunea, and Treating Lake ValkenburgWater

3.3.2 Data Pre-processing

Prior to model training, the above mentioned datasets were prepared and pre-processed. Initially, all sensor data were resampled to a common resolution. As the ambition pursued in this proof-of-concept was to develop an early warning system for reversible fouling, to optimise the backwashing operations, the models are expected to make predictions for short-term dynamics in the order of minutes, i.e., at high granularity. Therefore, a granularity of 1 minute was adopted for the proof-of-concept data-driven models. The high granularity TMP data from membrane module 7 and 8 were down sampled[1]. The sensor measurements of turbidity, temperature and flowrate were upsampled[2] from 15 minutes to 1 minute. This was conducted by adopting the last measured value for the time window, until a new value is available. This was considered acceptable as it is expected that the dynamics of such measured variables will not vary significantly in such short-term dynamics. However, it is anticipated that the dynamics of the system witnessed over the longer time constants and their underlying influence to the predicted variable (TMP) can be relevant for the models to learn. Such relationships is expected to be captured by inputting longer durations of data (in the order of hours) for the iterative training within the optimisation framework and by providing sufficient training examples (in the order of months).

As discussed in Section 3.3.3 and Section 3.4, different approaches were tested for training and identifying good performing neural networks and machine learning models with an objective to forecast the TMP values or the derivative of TMP. In all cases, the environmental and operational data were utilised as input. For the cases of using neural network models, a total duration of ~5 months of data was used, from 03/26/2022 – 18/08/2022. In the machine learning framework (Section 3.4), the limiting factor in-terms of amount of data was the SAC measurements. While, a measurement campaign of 3 months, from 23/12/2022 – 31/03/2023 was conducted, effectively, ~2.5 months of data was available due to the occurrence of certain technical failures resulting in missing data, both for the SAC Hach sensor and the operational SCADA data. Therefore, this amount of data was used in the analysis. In all AI modelling approaches utilising PWN data, the provided datasets were differentiated into a training set, used for model training, and a validation set, used to evaluated the trained models on an unseen dataset. For this purpose, the TMP dataset associated with membrane module 7 was used as the training set, and the TMP dataset associated with membrane module 8 was used as a validation set. This was considered as a robust method to ensure that the identified models are capable of performing well on parallel treatment modules, that though are operated similarly, they can possess differing system dynamics. The common measured WQ variables on the feedwater were considered to be the same for both membrane modules. For each approach, specialised data preparation and feature engineering was required based on the methodology adopted. Further details have been provided in the associated sub-section.

3.3.3 Neural Network Models as Potential Models in an Early-Warning System

In this study, neural network models were utilised with the ambition of forecasting the reversible fouling, via the means of predicting the TMP or the increase in TMP over time. This has been envisioned as the first and most important component of the proof-of-concept early warning system for UF membrane reversible fouling. Two AI modelling approaches were pursued and evaluated based on the models capabilities of learning the full-scale data inputted and providing satisfactory predictions. The two approaches are as follows:

- Modelling Approach #1: Univariate TMP modelling and recursive predictions.(Section 3.3.5)
- Modelling Approach #2: Forecasting short-term increase in TMP over filtration cycles. (Section 3.3.6)

As the primary focus is to forecast the reversible fouling, via the increase in TMP, the models are trained using higher granular data, as detailed in Section 3.3, with the intention for the models to learn the short-term dynamics of the system that can in turn provide support for rapid decision-making. Both modelling approaches utilised specialised AI modelling technologies and require their own data preparation and feature engineering to setup the model training and experimentation. This has been detailed further in the below sections.

[1] Process of decreasing the sampling rate or reducing the number of samples in a dataset.

[2] Process of increasing the sampling ate or the number of samples in a dataset.

3.3.4 Description of Model Architectures

The models trained contained a combination of Long Short Term Memory (LSTM) and dense layers. LSTM layers, that were initially introduced by Hochreiter & Schmidhuber (1997), are a subset of Recurrent Neural Networks (RNNs) that are known to be efficient in learning long-term dependencies within data. An LSTM cell within the layer are more complex than conventional dense layers as they include various gates to regulate the flow of temporal information. A standard structure of an LSTM cell has been provided in Figure 9. An LSTM cell contains a forget gate (f), which determines how much information from the previous hidden and cell states will be removed, an input gate (i) that determines how much current information will be kept after updating the current state using the cell update state (C). Finally, the output gate (o), controls the information outputted based on the internal cell state. All gates are defined as linear relationships which utilises the inputs, recurrent information from previous cell states, and corresponding weights and biases terms for each gate. Typically, within an LSTM cell, a sigmoid activation function is used for the recurrent related information and the hyperbolic tangent function is used when updating the cell state.

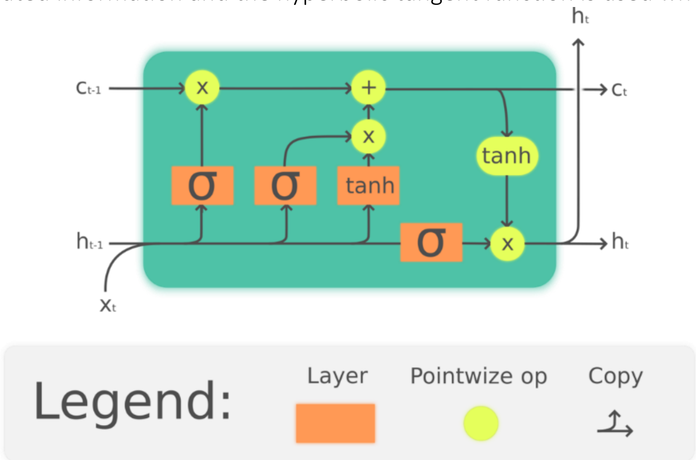

Figure 9 Standard Long Short Term Memory (LSTM) cell (Source: Image by Guillaume Chevalier under CCA 4.0)

3.3.5 Modelling Approach #1 – Univariate TMP Modelling and Recursive Predictions

In this modelling approach, historical TMP values at a high granularity (1 minute) were utilized to generate 1-step ahead predictions for the same TMP variable. This approach can be considered as a more simple baseline method where the potential of LSTM-Dense layered models to grasp temporal information and autocorrelation dynamics within TMP, are explored. Furthermore, these models were applied recursively, where the predictions were fed back into the model to make subsequent predictions, allowing for forecasts over a longer horizon. Various model architectures were trained with this data setup and subsequently assessed for their capabilities in making both 1-step ahead and recursive predictions. Given that a model architecture containing LSTM layers needs to learn from temporal information within the dataset, a fixed amount of historical input must be provided. For this investigation, an input of 54 minutes, roughly equivalent to 3 filtration cycles based on full-scale operational settings, was chosen based on a preliminary trail-and-error process and to also account for computational capacity. Furthermore, the TMP values that denoted backwash events were not removed prior to model training and validation, in order to maintain the temporal continuity of the dataset and to prevent gaps in the dataset.

3.3.6 Modelling Approach #2 – Forecasting short-term increase in TMP over filtration cycles

This modelling approach can be considered more comprehensive and involved, as compared to modelling approach #1. As discussed earlier, reversible fouling is typically associated with the increase in TMP within the filtration cycles. This can be identified through the values associated with the initial and final TMP of a given filtration cycle. Therefore, in this modelling approach, LSTM-Dense layered models are trained to learn the historical and temporal dynamics provided via environmental and operational data to forecast the initial and final TMP values of subsequent filtration cycles. The input data included the feedwater turbidity, temperature and flowrate, and the TMP measured in the membrane module. However, more advanced data preparation and feature engineering was required to identify the initial and final TMP values of filtration cycles. This is due to the fact that, while the filtration cycles are operationally set to be 18 minutes, the filtration cycles lengths witnessed in the high resolution sensor data does not necessary represent such a setting, and the cycles can be seen to be shorter or longer. Such uneven lengths of filtration poses a challenge in conducting a straightforward data processing method to identify the initial and final TMP of a filtration cycle. This was addressed by developing a semi-automated method, where the backwash events were first detected within the dataset. This was done by first calculating the derivate of the TMP for the duration of the data. An example of the TMP derivate time series has been provided in Figure 10.

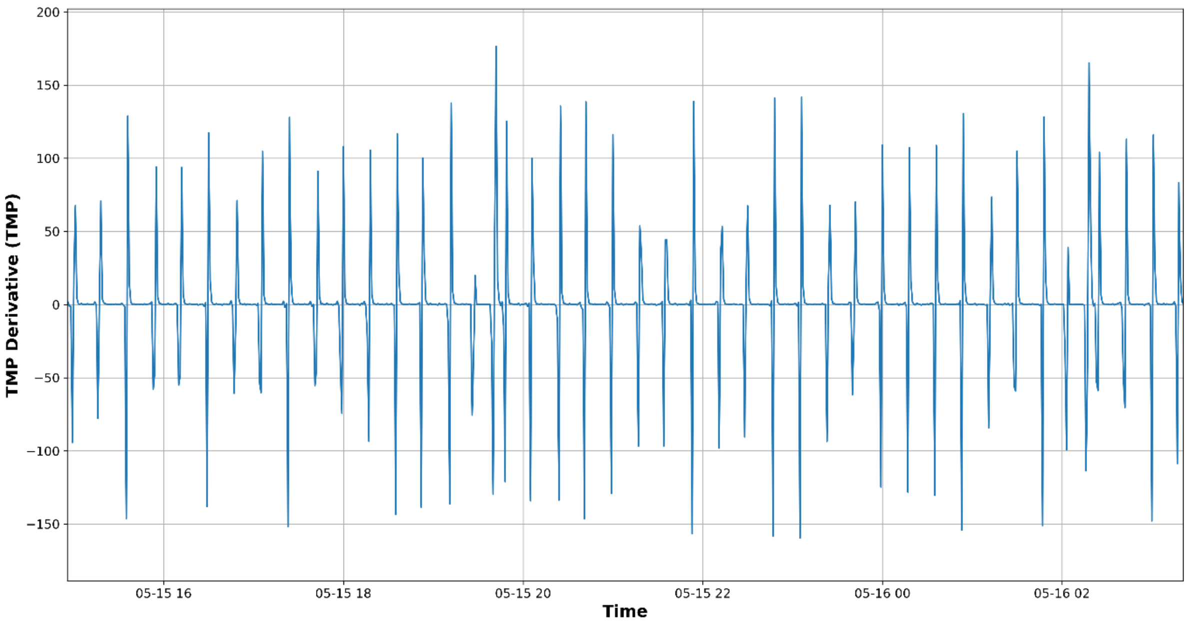

Figure 10 TMP Derivative calculated as a first step in identifying backwash events in highly granular TMP data

As it can be seen, the majority of the calculated derivatives reside close to 0, with specific spikes being seen in the positive and negative y-axis directions. This spikes are associated with a sudden drop towards highly negative TMP when a backwash is conducted, and rise back towards the more normal TMP ranges when the backwash is completed. To automate the process of identifying these events, a threshold detection based method was used, where a lower and upper threshold values were provided. The TMP derivative values that fall outside this range, where then flagged to be a backwash event. The lower and upper threshold values used for the TMP derivatives were -10 kPa and 10 kPa, respectively. The flagged timesteps where then utilised in the original TMP dataset to identify the backwash events. An example of the outcome of such a method has been provided in Figure 11. For each backwash event, the TMP value that precedes the backwash and the TMP value that follows, are identified. These values denote the final TMP of the preceding filtration cycle and the initial TMP of the subsequent filtration cycle, respectively.

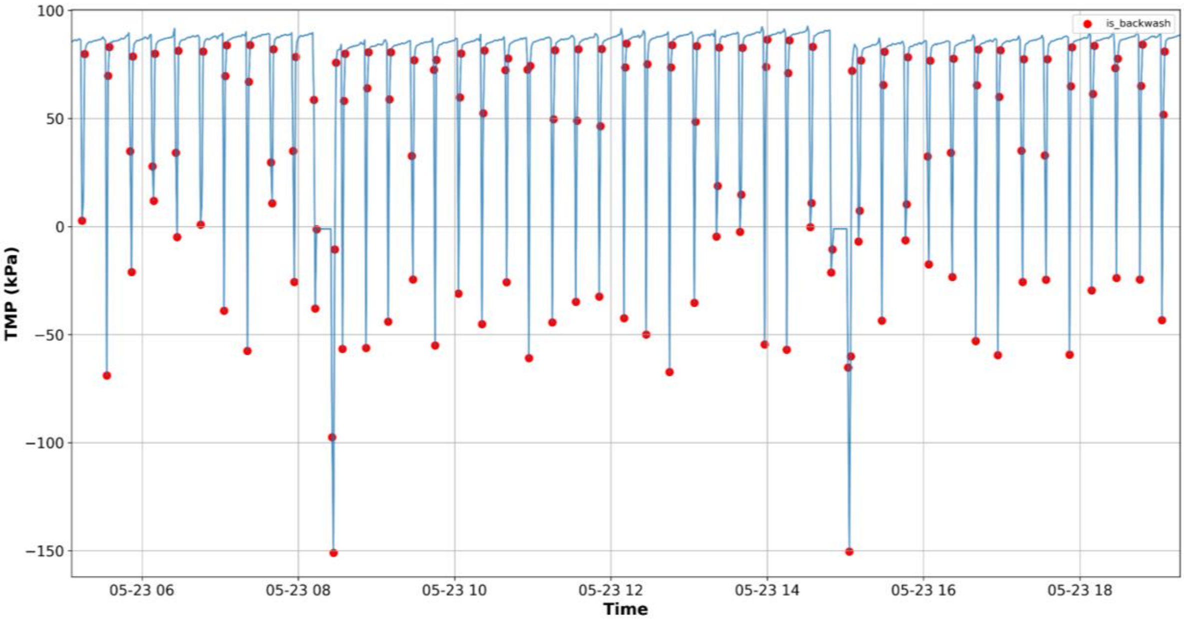

Figure 11 Backwash events identified in the TMP dataset as depicted by the red markers

With the initial and final TMP values identified, the datasets were then prepared into sequences. In one sequence, historica l input of 54 minutes (~3 filtration cycles) that precedes a given filtration cycle was identified as the temporal window for all the input variables, and were paired to the initial and final TMP of the same filtration cycle. Finally, models were trained to forecast 1, 2 and 3 filtration cycle ahead. Therefore, for each case, 2, 4 and 6 values were predicted, respectively. 3 filtration was the maximum cycles chosen as increasing the amount of cycles to forecast lead to significant reduction in training data available. Additionally, the best performing model where PWN data was used for the training and validation, was also tested on the Dunea data that relates to another water source, to assess their ability to generalize learning of membrane fouling phenomena and their capacity to provide accurate predictions for differing systems.

3.3.7 Model Trainings and Selection Procedure

To identify trained LSTM-Dense models providing accurate predictions, various models of different sizes and complexity were trained. For both modelling approaches, the number of hidden layers was restricted to 2, and a grid search was conducted to identify the number of neurons per layer. All models training were conducted using the stochastic gradient descent (SGD) optimisation while using the Adam optimiser and a specified loss function. The models were trained for a fixed number of epochs whole considering computational capacity available. The learning rate was scheduled using a step decay function, which exponentially reduced the learning rate after fixed number of epochs. This was incorporated to prevent the model loss to oscillate and be stuck in local minima during the optimisation process. The batch size for each iteration of the gradient descent was determined based on trial and error. All model developments and training were conducted using the Python software library of TensorFlow (Abadi et al., 2016). In Table 4, the hyperparameter choices for the model trainings have been provided.

Table 4 Hyperparameter choices for neural network model trainings

Hyperparameter	Value/Choice
# of epochs	100
Optimiser	Adam
Learning rate	Initial = 0.001 Step decay rate = 0.5 Number of epochs = 10

Activation function	LSTM layer = tanh Dense layer = ReLu
Batch size	Approach #1 = 128 Approach #2 = 32
Hidden layer 1 (LSTM)	16, 32, 64, 128 (based on grid search)
Hidden layer 2 (Dense)	16, 32, 64, 128 (based on grid search)

3.4 Random Forest Modelling to Evaluate SAC Parameter's Importance

Random forest (RF) is a supervised learning ensemble method based on bagging and feature randomness that combines the output of multiple decision trees to reach a single result. Such models can be used for classification and regression problems. RF are known to be efficient to train that can learn complex data and provide accurate results. Additionally, RF are considered as more interpretable models due to the utilisation of various decision trees that denote specific data samples within the dataset. As a result, RF models can be used to determine the importance of input variable or feature importance, used to make a prediction of a given target variable. This can be conducted using a method called permutation importance. In this technique input variables are permuted individually and the resulting impact in the model performance is measured. The degradation in the model performance, quantified by the decrease in a performance metric, is attributed to the importance of the given variable.

To determine the SAC parameter's importance in predicting reversible fouling and its ability to explain the membrane fouling behaviour in short-term dynamics of a full-scale operational plant, a RF model is trained using the dataset associated with the membrane module 7 of the Heemskerk UF installation. The model was also tested on the data for membrane module 8, which served in this case as an out-of-sample set. To identify the best model, a random search was provided for a grid of RF specific hyperparameters. The range of the values and the hyperparameters are provided in Table 5.

Table 5 RF Hyperparameters Ranges for Random Search Grid Used in Cross Validation

RF Hyperparameter	Range/Choices	Number of options
Number of estimators	10 – 100	50
Maximum features per split	'log2' or 'sqrt'	-
Maximum depth of tree	2 – 30	29
Minimum number of splits	2 – 10	10
Minimum samples required to split a node	1 – 10	10
Maximum number of leaf nodes	10 – 100	110
Bootstrap	True or False	-

A total of 1000 iterations were permitted for the random search. Additionally, cross validation, using 5 folds was used, where the data divided into 5 parts, where 4 parts are used for training and 1 for validation. The average score of all folds is used as the final performance.

Specifically, the feed water turbidity, temperature, and flowrate, along with the SAC parameter values were used as input. The target variable to predict was the derivative of TMP (TMP difference at two consecutive timesteps). The datasets were maintained at a granularity of 15 minutes. Permutation importance was carried out to determine the importance of each input variable, including the SAC parameter, to assess its importance in predicting the change in TMP over time.

3.5 Model Performance Metrics

The performance of the different model structures and modelling approaches were evaluated by comparing the predictive performance on the training set and the validation set, i.e., unseen data not used during the training process. To this aim, the Root Mean Squared Error (RMSE), which penalises large errors is used:

$$RMSE = \sqrt{\frac{\sum_i^N (y_i - \hat{y}_i)^2}{N}}$$

where, $\hat{y}_i$ and y_i are the predicted and measured value at time instant i respectively, and N is the number of considered data points. Furthermore, the performance metric Coefficient of Determination (CoD or R^2) was used:

$$R^2 = 1 - \frac{\sum_i^N (y_i - \hat{y}_i)^2}{\sum_i^N (y_i - \bar{y})^2}$$

where $\bar{y}$ is the average value of observed data calculated over N data points.

4 Results and Discussion

4.1 Screening of water quality parameters to predict fouling

4.1.1 Reversible and non-backwashable membrane resistance build up on different locations and seasons

The reversible resistances build-up calculated from the laboratory UF tests are presented in Figure 12 with its respective deviation. The highest resistance observed was at Andijk in Autumn, with a median value of 3 x 10^{10} $1{\cdot}m^{-1}{\cdot}h^{-1}$, which is substantially (6 times) higher compared to the samples taken in winter, spring and summer, which were of the same order. Valkenburg showed lower resistance values than Andijk within 1.2-4.6 x 10^{9} $1{\cdot}m^{-1}{\cdot}h^{-1}$. As expected, from the three locations, Heemskerk showed the lower reversible resistance build up in the range of 2.5-5.3 x 10^{8} $1{\cdot}m^{-1}{\cdot}h^{-1}$ due to its pretreatment. However, the samples tests showed the highest deviation within the replicates (1.2x 10^{7} $1{\cdot}m^{-1}{\cdot}h^{-1}$). Furthermore, it was shown that the water samples from the spring exhibited the lowest reversible resistances for all types of water.

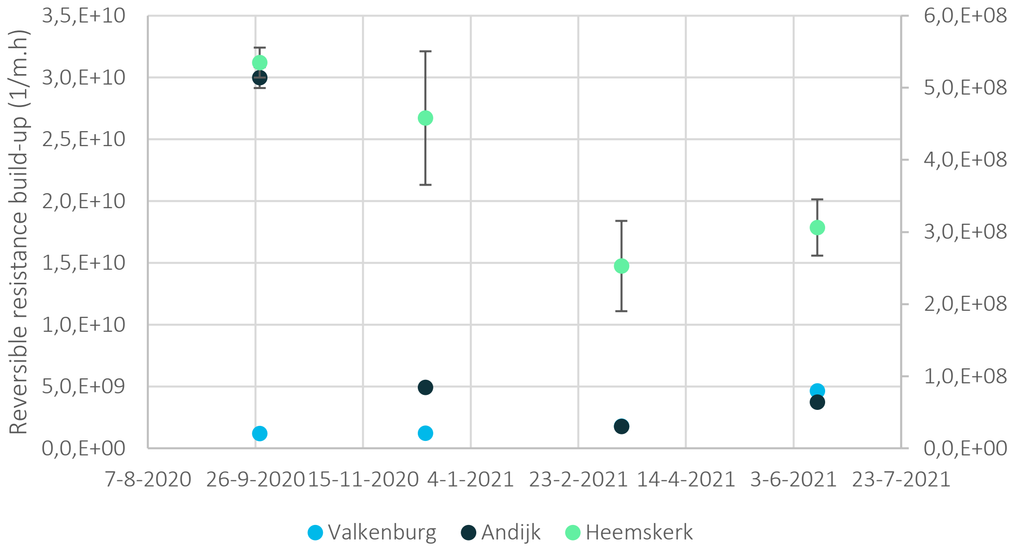

Figure 12 Reversible resistance build up with all samples from the different locations/waters during the 4 seasons (Autumn, Winter, Spring and Summer). Right y-axis for Heemskerk (pretreated water)

Likewise, the average determined non-backwashable resistance build up within the mini-UF test are presented in Figure 13. In Andijk the average irreversible resistances were in the range of 4.4 – 6.3 x 10^{7} $1{\cdot}m^{-1}{\cdot}h^{-1}$, with samples from spring being the less prompted to fouling. A similar trend (declining from Autumn to Spring and increasing in summer), after the pretreatment, was observed at Heemskerk with average non-backwashable resistances in the range of 0.6 – 2.8 x 10^{7} $1{\cdot}m^{-1}{\cdot}h^{-1}$. However, this same trend was not observed with lake Valkenburg raw water, in which the summer sample showed the highest non-backwashable resistance buildup of an average 1.0 x 10^{8} $1{\cdot}m^{-1}{\cdot}h^{-1}$. Accordingly, the raw water with the less ultrafiltration fouling potential within the majority of the seasons (Autumg to Spring) was lake Valkenburg.

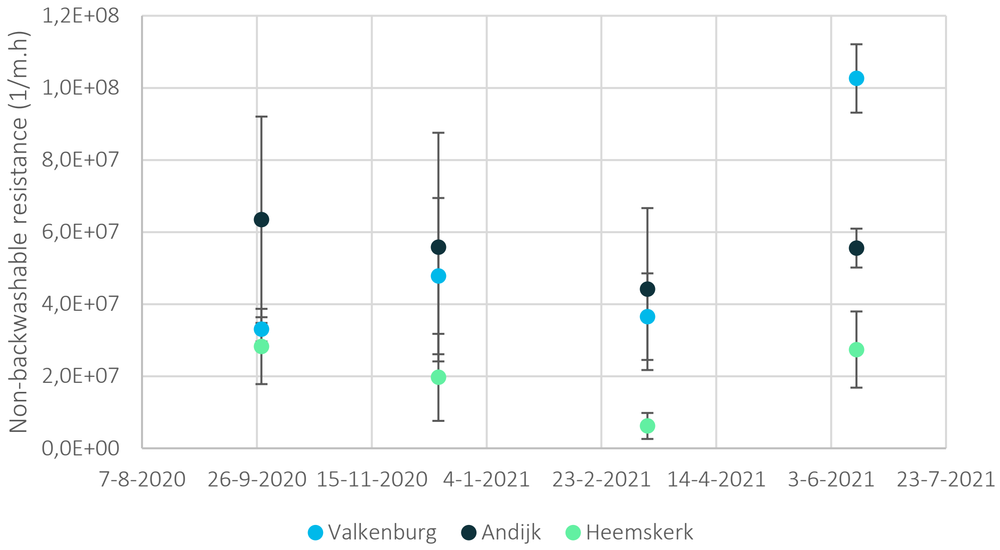

Figure 13 Non backwashable resistance build up with all samples from the different locations/waters during the 4 seasons (Autumn, Winter, Spring and Summer). Right y-axis for Heemskerk (pretreated water)

4.1.2 Principal Compound Analysis (PCA) of the water samples at different locations

A PCA analysis from the samples and water quality data associated to them is presented in Figure 14. A. It can be observed that the three water types at the locations Valkenburg, Andijk and Heemskerk can be regarded as three different groups. The lake Ijssel raw water (orange) and lake Valkenburg raw water(green) are not comparable, even though both surface water bodies originate from river Rhine. It can be seen that the Andijk and Heemskerk water samples, both coming from the IJssel lake, are very different from Valkenburg. Ijsel lake is shallow (~10 m) in comparison with Valkenburg (up to 40 m).
The PCA loading plot (Figure 13. B) showed how water quality parameters, resistance build up and seasonal effect influences the two principal components. This shows how parameters are correlated, suggesting that the water quality parameters of highest correlation with the principal component 2 are biopolymers BP concentration, Spectral Adsorption Coefficient SAC, MFI-UF value, Suspended matter (SM) concentration, MFI 0.45, Saturation index SI and total manganese concentration. These parameters are predominantly related to particulate matter and high organic dissolved matter.

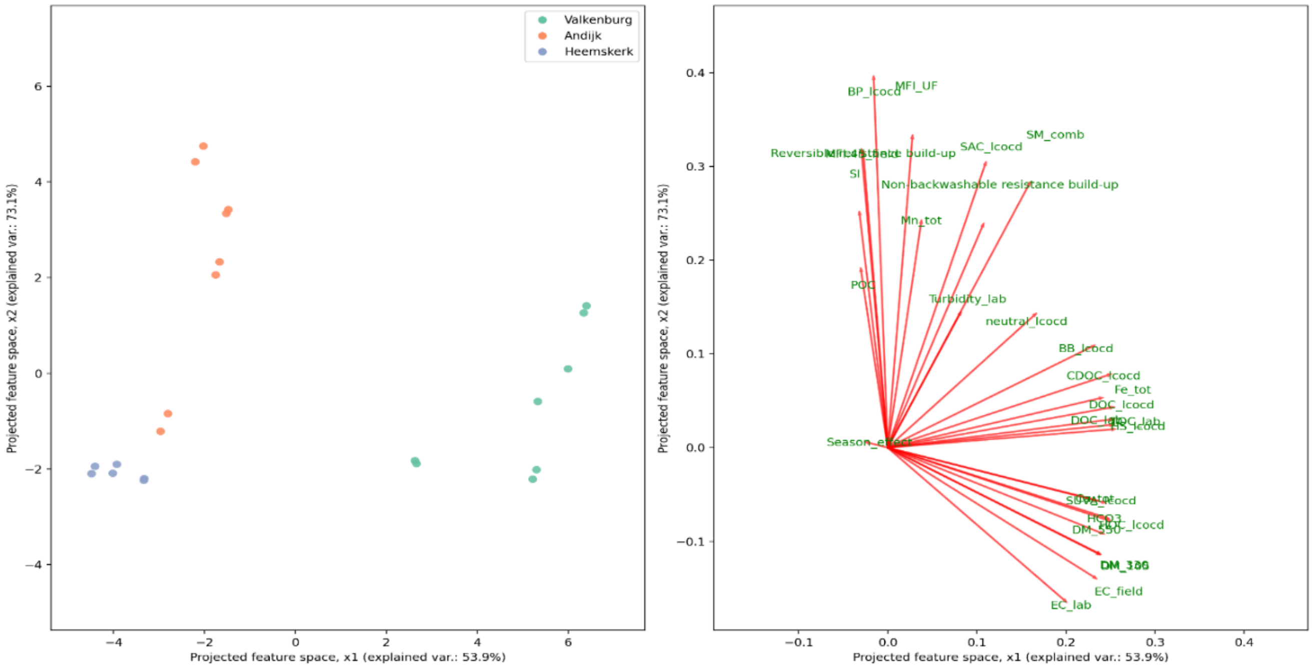

Figure 14 PCA analysis of A. Surface water samples from different locations B. All water quality parameters measured, resistance build up and , of measured water quality parameters.

4.1.3 Correlation analysis of measured water quality parameters and membrane resistance build-up

From all the water quality parameters results from all the samples taken at Valkenburg, Andijk and Heemskerk, correlation factors with reversible fouling build-up (blue) and non-backwashable fouling build-up (orange) were determined (Figure 15). Based on the correlation factors with water quality parameters it can be inferred that biopolymers, MFI.45, MFI UF, spectral adsorption coefficient, suspended matter, neutrals are the parameters with the highest correlation with fouling or resistance build up from the whole data set.

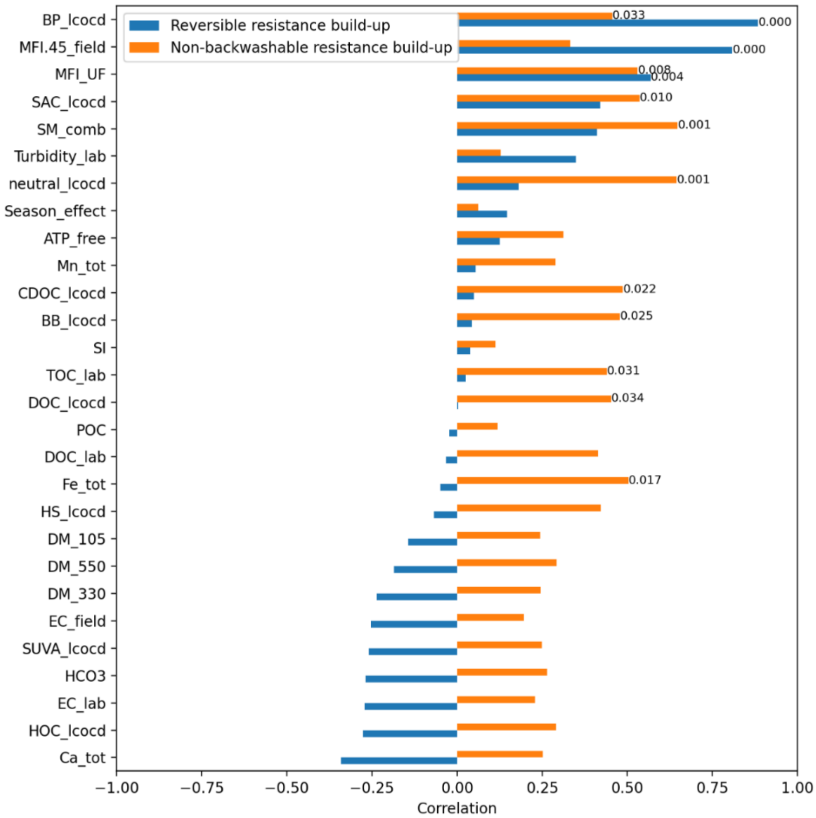

Figure 15 Overview of calculated correlation factors with reversible fouling build-up (blue) and non-backwashable fouling build-up (orange) of all tested water quality parameters (BP = biopolymers, MFI 0.45µm, MFI UF, SAC: Spectral adsorption coefficient, SM: Suspended matter, Turbidity, Neutrals, Seasonal effect, free ATP, Manganese, Chromatographical dissolved organic matter, Building blocks, Saturation index, Total Organic carbon, Dissolved organic carbon, Particulate organic matter, Iron, humic substances, dry matter after 105 degrees, dry matter after 550 degrees, dry matter after 330 degrees, Electric conductivity, Specific UV adsorbance, Hydrogen carbonate, Hydrophilic organic matter and Calcium).

The statistical analysis of the results of the water quality parameters data set after applying a selection criteria (significance of P<0.015 in at least one of the correlations with reversible and non-backwasable resistance build up) with the most highly correlated and significant water quality parameters are shown in Figure 16. For both reversible- and non-backwashable resistance build-up, white-colored numbers indicate the calculated correlation factors where numbers closer to integers 1.0 or -1.0 indicate a stronger correlation. To support evaluation of the calculated correlation factors, the significance of the observed relation is expressed as a P-value which is indicated by the cell color (green being the most significant). The lower the P-value (closer to black), the higher the significance of the calculated correlation factor. The actual data underlying this correlation calculations is presented in Figure 22 (Appendix II). The water quality parameters that did not meet the correlation-selection criteria are not further discussed.

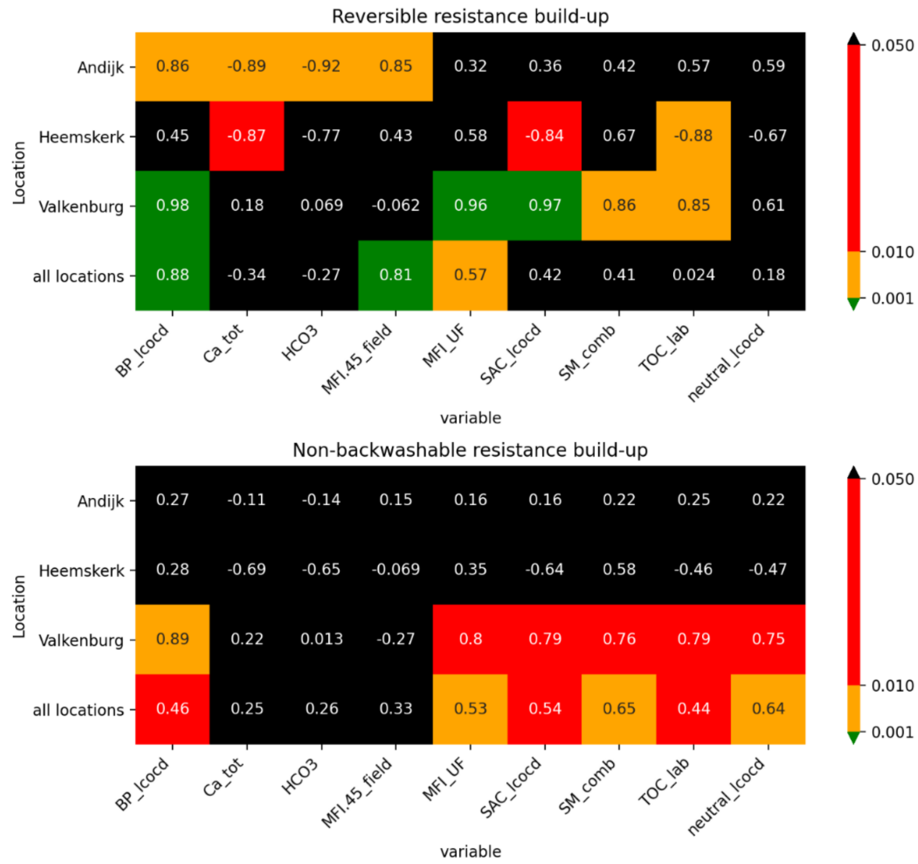

Figure 16 Overview of calculated correlation factors (white numbers) and their significance (color scale: P-value<0.001: Green (most significant), P-value<0.01: Orange, P-value<0.05: Red, P-value>0.05: Black (non- significant)) with respect to reversible- and non-backwashable resistance build-up on Pentair RX300 ultrafiltration membrane straws.

For sample Lake Valkenburg raw the water quality parameters biopolymers, spectral adsorption coefficient (SAC), MFI-UF, suspended matter and total organic carbon (TOC) showed both high correlation factor (>0.84) and high significance (P<0.010) towards the calculated reversible resistance build-up. The neutrals showed some correlation factor (0.61), but no significance (P>0.050). Regarding to the non-backwashable resistance build-up, the correlation with the biopolymers was most pronounced (correlation factor 0.89, 0.001<P<0.010). MFI-UF, SAC, TOC, suspended matter and the neutrals also showed strong correlations (>0.74) with significance (0.050<P<0.010). There parameters are in agreement with the expected, since reversible fouling is (roughly) related to particulate fouling and cake-layer build-up, while non-backwashable fouling is (roughly) related to 'sticky' fouling or foulant adsorption.
For sample Lake IJssel raw (Andijk) the water quality parameters biopolymers, calcium, bicarbonate and MFI0.45µm show both high correlation factor (>0.84 / <-0.88) and high significance (0.001<P<0.010) towards the observed reversible fouling build-up. With respect to the non-backwashable resistance build-up, none of the selected water quality parameters showed a high correlation (>0.50 / <-0.50) or significance (P>0.050).
For sample Lake IJssel pre-treated (Heemskerk) the water quality parameters TOC, calcium and SAC showed both high correlation factor (<-0.83) and significance (0.050<P<0.001) towards reversible resistance build-up. Bicarbonate, (-0.77), suspended matter (0.67), neutrals (-0.67) and MFI_UF (0.58) show some correlation, but no significance (P>0.050). For the non-backwashable resistance build-up calcium, HCO3, SAC and suspended matter show a strong correlation (>0.57 / <-0.63) but all these were not statistically significant (P>0.050). It can be inferred that Biopolymers are removed by the pretreatment sand filtration/activated carbon filtration, since correlation is high in both Ijssel lake and Valkenburg lake raw waters but lower and less significant in Heemskerk pretreated Ijssel water. The same trend is observed for MFI 0.45. Apart from these two parameters, both raw water types show no similar

high & significant correlation. In the case of SAC, it showed high correlation and significance in Valkenburg lake raw water and Heemskerk pretreated water. These three parameters seem to be the preferable to be selected for an online monitoring and be used as an input for an early warning system. Biopolymers cannot be measured online, while MFI 0.45 and SAC can be measured semicontinously (within a certain interval of time). However, SAC is the parameter than is practically easier to be measured with the use of a probe. Therefore, it was selected for further monitoring at a full-scale UF application, at the location Heemskerk, in which also showed a high correlation (-0.84) and significance (P<0.05).

4.2 Online SAC monitoring

The spectral absorption coefficient was monitored using ….. during a period of approximately 3 months at the header of the UF full scale installation at Heemskerk, PWN. The results showed that during this period the SAC values varied between a range of 6.0 and 9.0 m^{-1} (Figure 17). This variation is relatively small and shows that the water quality after pretreatment of coagulation, flocculation, sedimentation, rapid sand filtration and partial (20%) activated carbon filtration remained similar during this season of operation. Based on the operational data and operation engineers, not notable disturbances of the ultrafiltration process was observed during this period in any of the UF membrane skids.

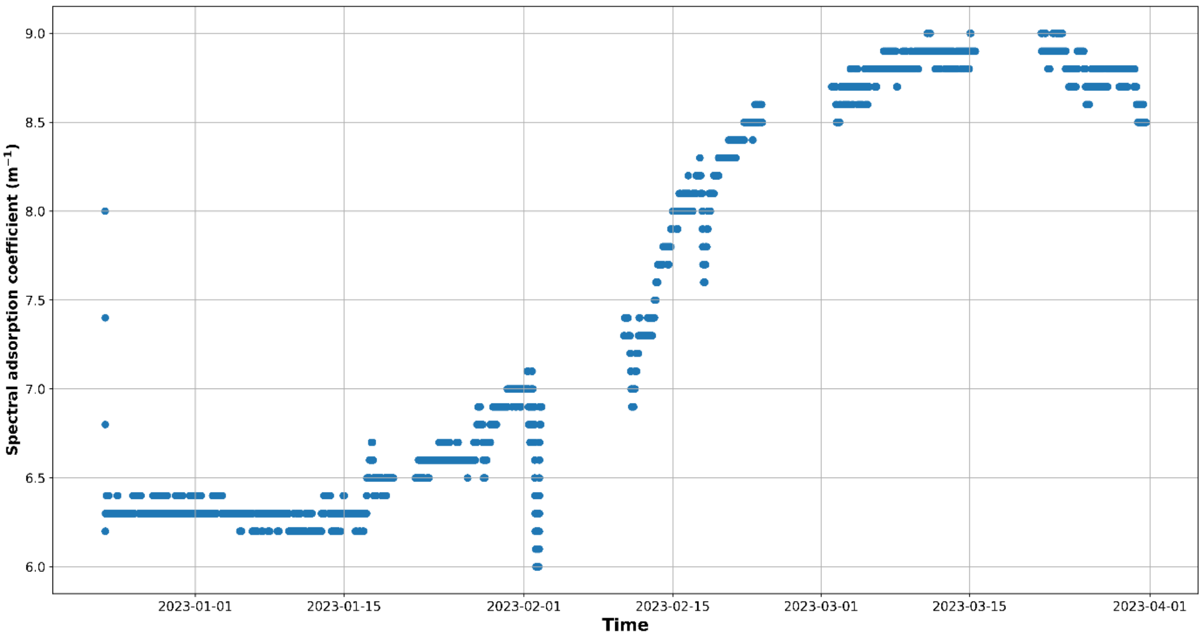

Figure 17 SAC values during the period of monitoring online. Empty spaced indicated days in which the memory of the SC4500 controller was full and data was not recorded properly.

The latter infers that for the purpose of supporting an AI model, the minimal changes observed from the inlet water quality and the operational behaviour during this period, will likely result in a low significance and further long evaluation of the SAC monitoring during the four seasons of the year is recommended.

4.3 Neural Network Modelling for forecasting TMP from UF Membranes

4.3.1 TMP-Only Modelling and Recursive Predictions

A grid search was conducted that trained models with varying number neurons for the 2 layers. All models trained provided very high performance in the training and validation dataset, with an R2 value of > 0.95, when performing 1-step ahead predictions. A summary of the model results can be found in (Table A3 1). In Figure 18, a time series plot that illustrates the 1-step ahead prediction made by the LSTM (16) – Dense (64) model is provided. As it can be seen, the prediction line follows the trends and the overall dynamics of the filtration cycles very well. The model satisfactorily predicts the increase in TMP in a filtration cycle. However, the predictions from the model in some instances can be considered unphysical or unfeasible. For example, for various filtration cycles, the model tends to predict a higher TMP values even before the cycle has completed. Such a behaviour might be considered expected to occur as data-driven models are black-box in nature and do not possess any information on the underlying physics of the system or the membrane fouling phenomena. The occurrence of the backwash events in the TMP values appears to also cause the reduced accuracy and nonphysical predictions being made by the model. The model is attempting to learn the TMP dynamics with the filtration cycle while also learning the sudden spikes and drops due to the backwash. Furthermore, only the TMP data is being used as input to make predict future values of the same variable. As a result, no other variables have been provided to the model that might explain the occurrence of fouling and the rise in TMP.

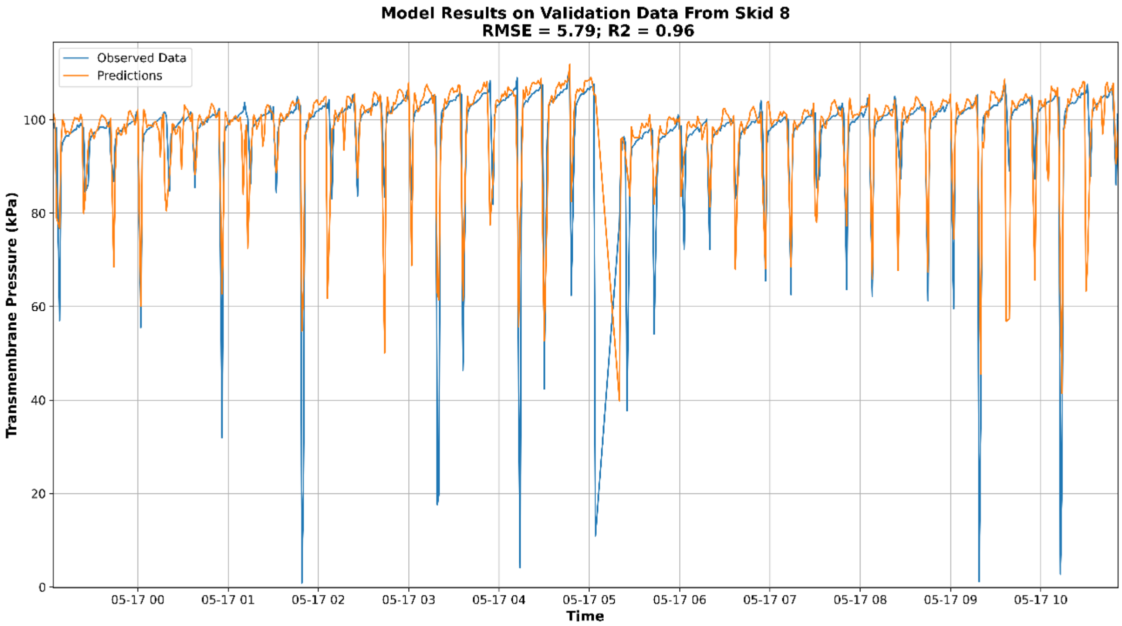

Figure 18 LSTM (16) - Dense (64) Model 1-step ahead TMP Predictions on the Validation Set. Blue line represents the observed data and orange line represents the predictions.

The model underwent testing to assess its ability to recursively predict transmembrane pressure (TMP) over a forecasting horizon, given the imperative need for these models to offer insightful early-warning support. A forecasting horizon of 54 minutes ahead (equivalent to approximately 3 filtration cycles) was employed, and an example is depicted in Figure 19. However, it is evident that the model struggles to rely on its own predictions for making further forecasts into the future. While it provides acceptable predictions for approximately 5 minutes, errors begin to accumulate, resulting in a significant deviation in the model's predictions, particularly during a backwash event. This leads to suboptimal predictions for the remaining duration of the horizon. This observation suggests that a univariate modelling approach of using the historical TMP data to predict future TMP values may have limitations when used within an early-warning system. To address this, consideration could be given to supplementing the method by incorporating additional variables as inputs, thereby providing more information on the apparent non-linear dynamics. In such an approach, the models trained can be used to predict the entire forecasting horizon in one-shot. Moreover, hybrid modelling approaches, incorporating physics-based equations and leveraging known domain knowledge on membrane fouling, can be integrated into the training process. This inclusion serves to enhance the explanation of the model results and introduces physical constraints to improve the overall performance of the model.

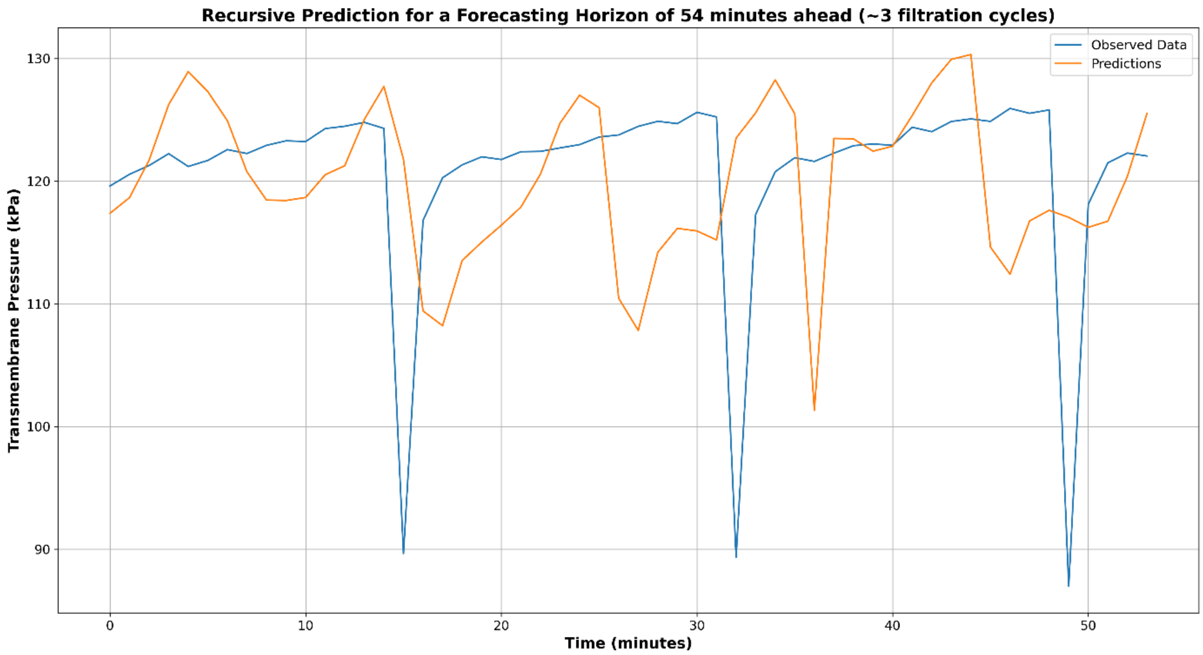

Figure 19 Recursive Predictions by the LSTM (16) - Dense (64) model on the Validation Set for a Forecasting Horizon of 54 Minutes Ahead and During a Potential Fouling Event.

4.3.2 Predicting TMP development between filtration cycles

The modelling approach described in Section 3.3.6 also involved performing a grid search where models of varying number of neurons per layer were trained. All models trained provided highly accurate predictions in singularly predicting the initial and final TMP for 1 filtration cycle ahead (Table A4 1), 2 filtration cycle aheads (Table A4 2) and 3 filtration cycles ahead (Table A4 3). Models conducting predictions for 3 filtration cycles ahead can be considered as more complex (due to outputting more values in a prediction) but more useful with respect to its usage in an early-warning system. The prediction of 3 filtration cycles represent the forecasting of the TMP increasing dyanmics witnessed roughly 54 minutes ahead (using the operational value of 18 minutes a filtration cycle). As shown in Table 6, the best performing model based on the R^2 values for 3 filtration cycles in the training and validation set was identified to be an LSTM (128) – Dense (32) model. This model provided high R^2 values but was not the largest model trained in the grid search performed and therefore provides a good solution in being accurate and not overly complex, which can lead to overfitting issues when faced with more unseen datasets.

Table 6 LSTM (128) - Dense (32) Model Performance Metrics in Conducting Initial and Final TMP for up to 3 Filtration Cycles in the Future

Layers		1 Filtration Cycle Ahead				2 Filtration Cycle Ahead				3 Filtration Cycle Ahead			
#1	#2	Train R^2		Validation R^2		Train R^2		Validation R^2		Train R^2		Validation R^2	
128	32	Initial	Final	Initial	Final	Initial	Final	Initial	Final	Initial	Final	Initial	Final
		0.99	0.99	0.98	0.99	0.94	0.94	0.94	0.94	0.94	0.94	0.94	0.92

Furthermore, in Figure 20, the scatter plots comparing the observed measurements and model predictions for the initial and final TMP values of all 3 filtration cycles have been illustrated. The plots suggests that the model provide highly satisfactory and accurate predictions, for all TMP ranges seen in the dataset, for both the training and validation sets. This suggests that model has learned the various environmental and operational conditions sufficiently.

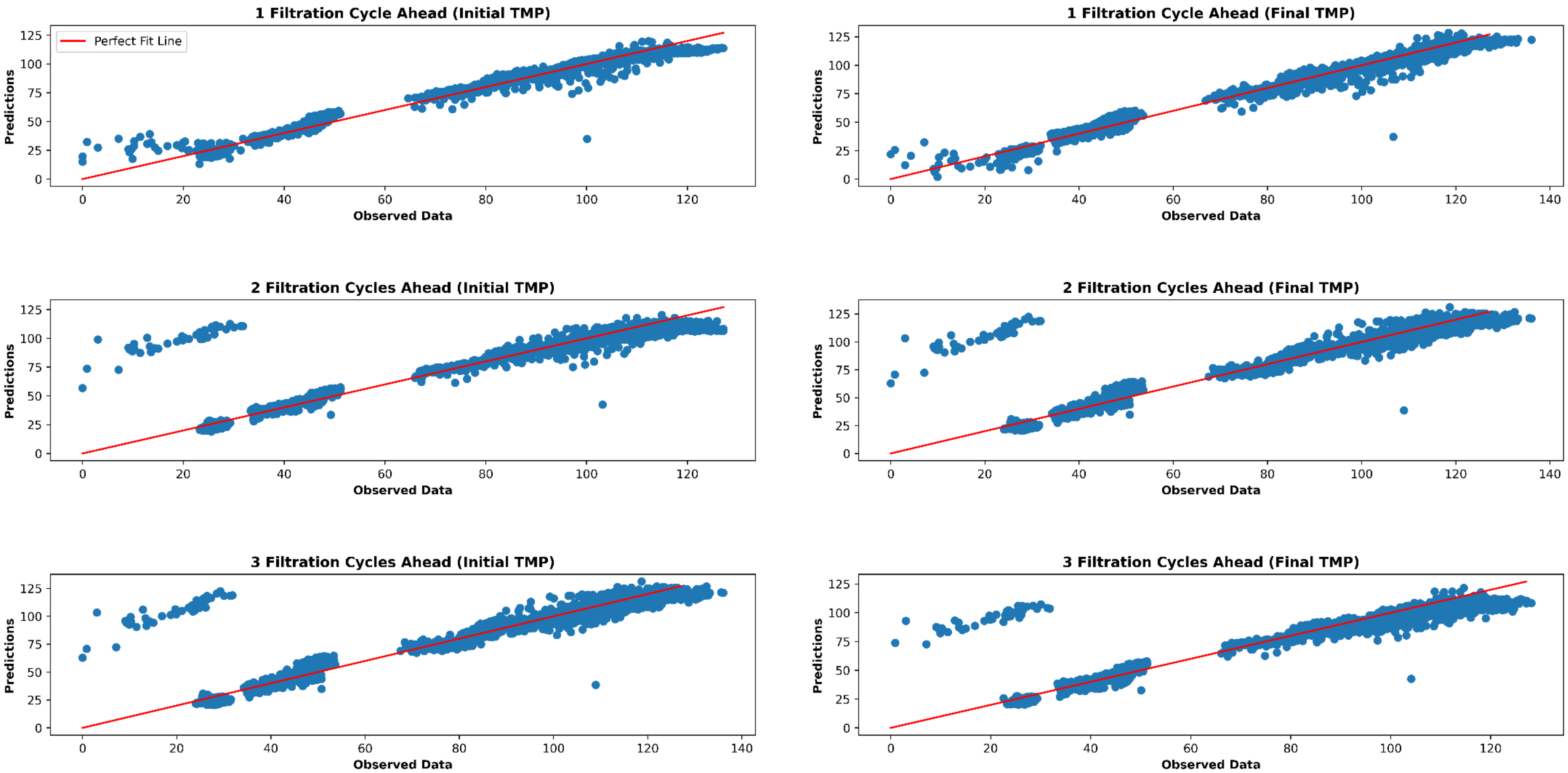

Figure 20 Scatter Plots of the Observed vs. Predicted for the Initial and Final TMP for up to 3 Filtration Cycles Ahead, using an LSTM (128) - Dense (32) Model

The results obtained from this modelling approach provides a promising outlook for using such a data preparation and model training technique to forecast more filtration cycles ahead. Typically for the early-warning system to provide meaningful insights to support predictive maintenance type operational decisions, one could require predictions ~8 hours ahead, which for the PWN case study, amounts to roughly 9 filtration cycles. However, the more filtration cycles ahead that are needed to be forecasted, the more historical input will be required. This can reduce the number of samples (filtration cycles) available for training. It is anticipated that with the current dataset available, predicting these many filtration cycles ahead could lead to lower R^2 performances. Therefore, an interesting follow-up to this methodology would be to focus on training such model using multi-year data of high granularity, which can provide sufficient amount of data to forecast, for example, 9 filtration cycles (18 outputs) ahead.

4.3.3 Generalisation capabilities of the neural network models to predict development in TMP

A preliminary investigation was conducted to test the generalisable capabilities of the best neural networks identified using the PWN data for training. This involves performing predictions utilising the data from the UF pilot installation that treated the source water received from the lake Valkenburg. For this test, the best performing neural networks in the modelling approach #2(result reported in Section 4.3.2) in predicting 1 filtration cycle ahead was used. The model chosen is an LSTM (16) – Dense (32) model. The ~2 weeks of Dunea data was pre-processed using the technique described in Section 3.4.3. However, unfortunately, the performance of the models on this alternative dataset is highly poor, where an R2 value of -2.04 and -1.20 was achieved for predicting the initial and final TMP values of 1 filtration cycle ahead, respectively. This suggests that the model trained on PWN data has only learned the system specific dynamics of the UF operations, and cannot generalise to another system, thereby indicating that the model is significantly lacking information on the non-linear dynamics related to UF membrane and the fouling phenomena. Furthermore, the filtration cycle length of the Valkenburg UF pilot is seen to be 25 minutes and more, which is longer than the UF installation at Heemskerk (around 18 minutes). Such a difference could suggest that the data pre-processing and feature engineering conducted to prepare the training set might not be interoperable. More in-depth evaluations are suggested to get further details on the causes behind the poor generalisable capabilities of the PWN neural networks. Furthermore, the development of hybrid models that can include certain domain knowledge on UF membrane operations in neural network training can lead to the capturing of processes that are common to many UF systems.

4.3.4 Importance of SAC for increasing prediction accuracy

As described in Section 3.4, a machine learning framework involving the training of a RF model on specific data that included the feedwater turbidity, temperature and flowrate, along with the SAC parameter data, which was collected in this project (Section 3.2). The target variable for the RF model is the TMP derivative (change in TMP over time). Based on the random grid search conducted using a 5-fold cross validation technique, the best performing model was identified, with the values of the hyperparameter provided in Table 7.

Table 7: Optimal Hyperparameters Identified for Best RF Model Trained Using 5 Fold Cross Validation

RF Hyperparameter	Optimal Value
Number of estimators	28
Maximum features per split	‘sqrt’
Maximum depth of tree	25
Minimum number of splits	5
Minimum samples required to be at a leaf node	1
Maximum number of leaf nodes	95
Bootstrap	True

The RF model was trained and validated using roughly ~2.5 months of data from the membrane module 7. The model achieved a RMSE and R^2 value of 1.41 kPa and 0.81, respectively, which indicated a satisfactory fit in predicting the TMP derivative. Owing to this result, it was considered feasible to perform the permutation importance technique (refer Section 3.3.8) to assess the importance of the SAC parameter in making the TMP derivative predictions. The technique was conducted 10 times for each input variable. The results of this feature importance study is illustrated in Figure 21, where the mean decrease in R^2 score is provided with black vertical lines denoting the standard deviation. The low standard deviation provides a high level of confidence in the acquired results. It can be seen that the feedwater flowrate that is an operational parameter, was calculated to be the most important input variable owing to the large decrease in the mean R^2 score and therefore accuracy of the model predictions. This signifies that the mode relies greatly on the flowrate to predict the change in TMP. The second most important input variable was seen to be the SAC parameter, with nearly a 45% decrease in mean R^2 accuracy seen when permutated. These results suggest that the SAC parameter may provide data-driven models the necessary predictive power in accurately forecasting the (change) in TMP values and therefore, contribute in the explanation of the underlying processes that causes UF membrane fouling. Temperature appeared to have much lesser influence in the RF model predictions. This can be expected as a very short duration of data accounting for roughly 1 season was available for the model training. Turbidity was considered to provide very minimal contributions in the RF model predictions.

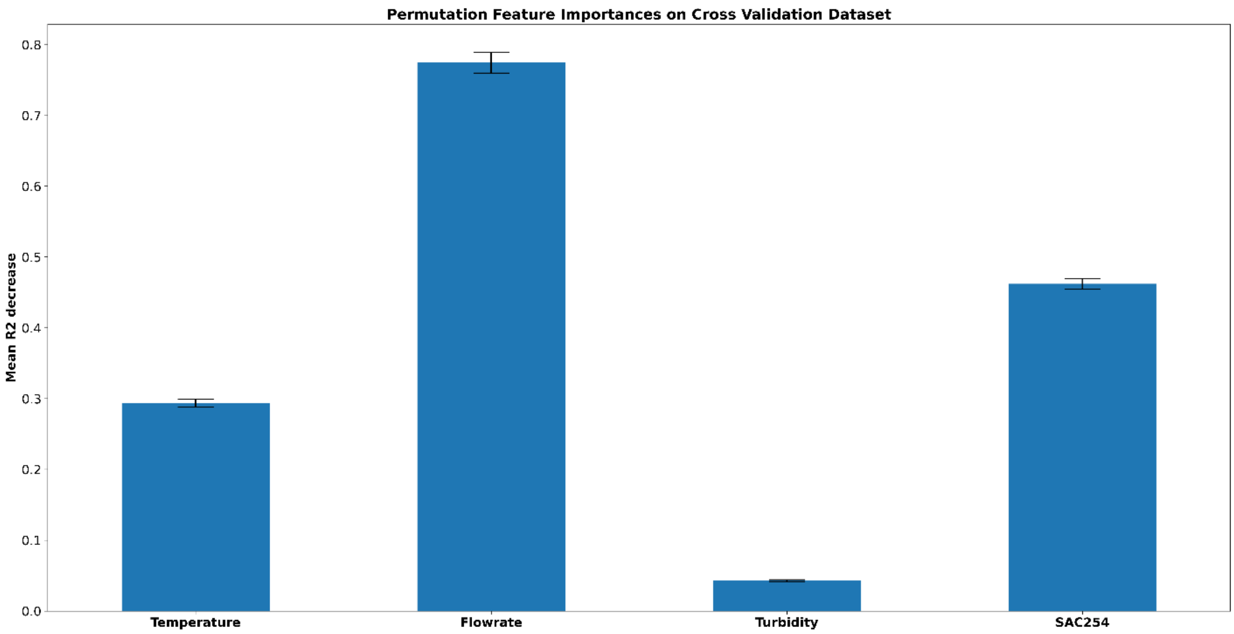

Figure 21 Mean Permutation Feature Importance Conducted on the Cross Validation Dataset Using the Trained RF Models. Black Vertical Lines Indicate the Standard Deviation

While the feature importance investigation provides some insights on the importance of the SAC parameter, certain considerations must be made. The RF model though providing a satisfactory fit of 0.81 for the cross validation dataset, yielded an average R2 score of 0.47. Such results signify that the model is overfitting on the training data which can signify that the feature importance results are not necessarily applicable to other environmental and operational conditions, which are not captured in the training dataset. Therefore, it is recommended that the results obtained from this study are further verified by conducting model trainings with a larger available dataset couple with more extensive feature engineering and evaluation.

5 Conclusions and Recommendations

The following conclusions on both the screening on water quality parameters and the AI modeling can be made out of this study:

- Significant seasonal variations in reversible resistances across Andijk, Valkenburg, and Heemskerk were found with the miniUF tests. Andijk, notably in Autumn, exhibited the highest resistance, 3 x 10^10 $1.m^{-1}.h^{-1}$, significantly exceeding the samples from the other seasons. Valkenburg consistently maintained lower resistances (1.2-4.6 x $10^{\wedge 9}$ $1.m^{-1}.h^{-1}$) than Andijk, while Heemskerk's pretreatment resulted in the lowest reversible resistance range (2.5-5.3 x $10^{\wedge 8}$ $1.m^{-1}.h^{-1}$), albeit with higher variability. Spring consistently featured the lowest reversible resistances across all locations or water types.

- Non-backwashable resistance build-up in mini-UF tests displayed trends in Andijk (4.4 – 6.3 x $10^{\wedge 7}$ 1. $m^{-1}.h^{-1}$) and Heemskerk (0.6 – 2.8 x $10^{\wedge 7}$ $m^{-1}.h^{-1}$), declining from Autumn to Spring. Notably, Valkenburg's raw water exhibited the highest non-reversible resistance build up with the water sample taken in summer (1.0 x $10^{\wedge 8}$ $1.m^{-1}.h^{-1}$). Consequently, lake Valkenburg demonstrated the least ultrafiltration fouling potential in the majority of seasons.

- The water quality parameters in Lake Valkenburg raw water, including biopolymers, spectral adsorption coefficient (SAC), MFI-UF, suspended matter, and total organic carbon (TOC), demonstrated high correlation and significance with reversible and non-backwashable resistance build-up. Notably, biopolymers exhibited the most pronounced correlation with non-backwashable resistance. In Lake IJssel raw water (Andijk), no parameters showed a strong correlation or significance with non-backwashable resistance build up. In Lake IJssel pre-treated water (Heemskerk), TOC, calcium, and SAC exhibited significant correlations with reversible resistance, while non-backwashable resistance build up lacked strong correlations. Biopolymers, MFI.UF 45 and SAC exhibited the stronger correlations for reversible resistance. Thereby, for a potential early warning system of reversible fouling build-up, SAC emerged as a practical parameter for online monitoring due to its ease of measurement (compared to MFI.UF45 and biopolymers), due to its shown correlation and significance, and was selected to be tested at full-scale UF installation at Heemskerk.

- Neural network models that were trained singularly on historical TMP data from the Heemskerk full-scale UF plant, to forecast the TMP data itself, exhibited very good accuracy when performing 1-step ahead predictions. However, these particular models when tested to perform recursive predictions (predictions inputted to further forecast over a time horizon), significant error accumulation was seen with the model performance deterioration approximately after 5 minutes.

- Based on exploration of the data, it was seen that the operational setting of a filtration cycle's duration is not consistently reflected in the time series data, and is seen to vary significantly. Therefore, a comprehensive and semi-automated data-preprocessing and feature engineering procedure was developed. This procedure effectively identified backwash events, enabling the extraction of initial and final TMP values for individual filtration cycles. These extracted data points serve as valuable targets for the training and identification of neural network models, ensuring a targeted approach to developing models that can be used within an early warning system.

- The neural network models, trained to forecast the rise in TMP over subsequent filtration cycles, were initially trained on data specific to the Hemskerk UF installation operated by PWN. To assess the model's generalization capabilities to other UF systems, preliminary tests were conducted using datasets from a different system – a UF pilot treating water from lake Valkenburg, operated by Dunea. Unfortunately, the models exhibited significantly poor performance when forecasting 1 filtration cycle ahead. Additionally, the data processing technique applied to the Dunea dataset encountered challenges in accurately identifying the initial and final TMP values of filtration cycles, resulting in a loss of data.

- To assess the importance of the SAC parameter in predicting the TMP derivative (change in TMP), a random forest model was trained using cross-validation, where the SAC parameter along with the water quality and operational parameters as input. An RF model scoring an R2 value of 0.80 was achieved. Based on an employed permutation feature importance method, the SAC parameter was calculated to be the second most important predictor, preceded by the feedwater flowrate and succeeded by the feedwater temperature.

- A forecasting model based on the operation of UF installations can provide not only advanced operational guidance by optimizing the backwashing and cleaning intervals (and linked optimal chemical consumption) in the future but also a major contribution to the security of supply of UF membrane installations in practice, resulting in a future more robust water purification for the project partners, that can be used and trained in future in other UF installations

As a future outlook, the following recommendations were formulated:

- Considering the minimal spectral absorption coefficient (SAC) variations observed (6.0 to 9.0 m-1) over a 3-month period in Heemskerk's UF full-scale installation, further long-term evaluation across four seasons is recommended. The consistent water quality of the pre-pretreatment suggests a low likelihood of significant changes during the tested seasons (Winter/Spring), indicating limitation in relying on a short-time data set of SAC recorded data for a complete AI model support.

- It was experienced that online datasets associated with UF membrane treatment installations require heavy investment of time and effort to ensure adequate data cleaning, pre-processing and feature engineering. Such data curation steps are crucial to ensure meaningful training datasets are created for neural network model trainings and to also achieve accurate predictions to potentially use the models within an early-warning system.

- The limited model performance from the univariate modelling approach, where historical TMP data was used to forecast the same variable, when tested to predict recursively suggests that additional variables should be utilised as inputs to provide more information on the apparent non-linear dynamics. If such an approach is considered, the models trained can be used to predict the TMP for the entire forecasting horizon in one-shot.

- The unphysical nature of the data-driven model predictions coupled with the models failing to generalise and accurately forecast the targets when tested for another UF pilot installation suggests that a hybrid modelling approach can be explored to address such challenges. In such a framework, physics-based equations can be incorporated into the data-driven models and the training process. This inclusion can leverage known domain knowledge on membrane fouling to enhance the explanation of the model results while introducing physical constraints to improve the overall performances of the models.

References

Abadi, M., Agarwal, A., Barham, P., Brevdo, E., Chen, Z., Citro, C., Corrado, G. S., Davis, A., Dean, J., Devin, M., Ghemawat, S., Goodfellow, I., Harp, A., Irving, G., Isard, M., Jia, Y., Jozefowicz, R., Kaiser, L., Kudlur, M., … Research, G. (2016). TensorFlow: Large-Scale Machine Learning on Heterogeneous Distributed Systems. https://arxiv.org/abs/1603.04467v2

Abushaban, A., Salinas-Rodriguez, S.G., Philibert, M., Le Bouille, L., Necibi, M.C. and Chehbouni, A. (2022) Biofouling potential indicators to assess pretreatment and mitigate biofouling in SWRO membranes: A short review. Desalination 527, 115543. https://doi.org/10.1016/j.desal.2021.115543

Al-Juboori, R.A. and Yusaf, T. (2012) Biofouling in RO system: mechanisms, monitoring and controlling. Desalination 302, 1-23

Alam, G., Ihsanullah, I., Naushad, M. and Sillanpää, M. (2022) Applications of artificial intelligence in water treatment for optimization and automation of adsorption processes: Recent advances and prospects. Chemical Engineering Journal 427, 130011

AlSawaftah, N., Abuwatfa, W., Darwish, N. and Husseini, G. (2021) A Comprehensive Review on Membrane Fouling: Mathematical Modelling, Prediction, Diagnosis, and Mitigation. Water 13(9), 1327

AlSawaftah, N., Abuwatfa, W., Darwish, N. and Husseini, G.A. (2022) A Review on Membrane Biofouling: Prediction, Characterization, and Mitigation. Membranes 12(12), 1271

ASTM (2019) Standard Test Method for Modified Fouling Index (MFI-0.45) of Water. ASTM D8002-15e1.

Bagheri, M., Akbari, A. and Mirbagheri, S.A. (2019) Advanced control of membrane fouling in filtration systems using artificial intelligence and machine learning techniques: A critical review. Process Safety and Environmental Protection 123, 229-252

Boerlage, S.F.E., Kennedy, M.D., Dickson, M.R., El-Hodali, D.E.Y. and Schippers, J.C. (2002) The modified fouling index using ultrafiltration membranes (MFI-UF): characterisation, filtration mechanisms and proposed reference membrane. Journal of Membrane Science 197(1), 1-21. https://doi.org/10.1016/S0376-7388(01)00618-4

Brehant, A., Bonnelye, V. and Perez, M. (2002) Comparison of MF/UF pretreatment with conventional filtration prior to RO membranes for surface seawater desalination. Desalination 144(1), 353-360. https://doi.org/10.1016/S0011-9164(02)00343-0

Chew, C.M., Aroua, M.K. and Hussain, M.A. (2017) A practical hybrid modelling approach for the prediction of potential fouling parameters in ultrafiltration membrane water treatment plant. Journal of Industrial and Engineering Chemistry 45, 145-155. https://doi.org/10.1016/j.jiec.2016.09.017

Corbatón-Báguena, M.-J., Vincent-Vela, M.-C., Gozálvez-Zafrilla, J.-M., Álvarez-Blanco, S., Lora-García, J. and Catalán-Martínez, D. (2016) Comparison between artificial neural networks and Hermia’s models to assess ultrafiltration performance. Separation and Purification Technology 170, 434-444. https://doi.org/10.1016/j.seppur.2016.07.007

Cui, Y., Gao, H., Yu, R., Gao, L. and Zhan, M. (2021) Biological-based control strategies for MBR membrane biofouling: A review. Water Science and Technology 83(11), 2597-2614

Curcio, S., Calabrò, V. and Iorio, G. (2006) Reduction and control of flux decline in cross-flow membrane processes modeled by artificial neural networks. Journal of Membrane Science 286(1), 125-132. https://doi.org/10.1016/j.memsci.2006.09.024

Delgrange-Vincent, N., Cabassud, C., Cabassud, M., Durand-Bourlier, L. and Laîné, J.M. (2000) Neural networks for long term prediction of fouling and backwash efficiency in ultrafiltration for drinking water production. Desalination 131(1), 353-362. https://doi.org/10.1016/S0011-9164(00)90034-1

Delgrange, N., Cabassud, C., Cabassud, M., Durand-Bourlier, L. and Lainé, J.M. (1998) Neural networks for prediction of ultrafiltration transmembrane pressure – application to drinking water production. Journal of Membrane Science 150(1), 111-123. https://doi.org/10.1016/S0376-7388(98)00217-8

Di Bella, G. and Di Trapani, D. (2019) A Brief Review on the Resistance-in-Series Model in Membrane Bioreactors (MBRs).

Floris, R., Nijmeijer, K. and Cornelissen, E.R. (2016) Removal of aqueous nC60 fullerene from water by low pressure membrane filtration. Water Research 91, 115-125. https://doi.org/10.1016/j.watres.2015.10.014

Galinha, C.F. and Crespo, J.G. (2021) From black box to machine learning: A journey through membrane process modelling. Membranes 11(8), 574

Guo, W., Ngo, H.-H. and Li, J. (2012) A mini-review on membrane fouling. Bioresource technology 122, 27-34

Huber, S. and Frimmel, F.H. (1992) A liquid chromatographic system with multi-detection for the direct analysis of hydrophilic organic compounds in natural waters. Fresenius' Journal of Analytical Chemistry 342(1), 198-200. 10.1007/BF00321726

Jermann, D. (2008) Membrane fouling during ultrafiltration for drinking water production: causes, mechanisms and consequences, ETH Zurich. 10.3929/ethz-a-005714271

Kennedy, M.D., Chun, H.K., Quintanilla Yangali, V.A., Heijman, B.G.J. and Schippers, J.C. (2005) Natural organic matter (NOM) fouling of ultrafiltration membranes: fractionation of NOM in surface water and characterisation by LC-OCD. Desalination 178(1), 73-83. https://doi.org/10.1016/j.desal.2005.02.004

Kimura, K., Hane, Y., Watanabe, Y., Amy, G. and Ohkuma, N. (2004) Irreversible membrane fouling during ultrafiltration of surface water. Water Research 38(14), 3431-3441. https://doi.org/10.1016/j.watres.2004.05.007

Koo, C.H., Mohammad, A.W., Suja', F. and Meor Talib, M.Z. (2013) Use and development of fouling index in predicting membrane fouling. Separation & Purification Reviews 42(4), 296-339

Kovacs, D.J., Li, Z., Baetz, B.W., Hong, Y., Donnaz, S., Zhao, X., Zhou, P., Ding, H. and Dong, Q. (2022) Membrane fouling prediction and uncertainty analysis using machine learning: A wastewater treatment plant case study. Journal of Membrane Science 660, 120817. https://doi.org/10.1016/j.memsci.2022.120817

Krippl, M., Dürauer, A. and Duerkop, M. (2020) Hybrid modeling of cross-flow filtration: Predicting the flux evolution and duration of ultrafiltration processes. Separation and Purification Technology 248, 117064. https://doi.org/10.1016/j.seppur.2020.117064

Li, L., Rong, S., Wang, R. and Yu, S. (2021) Recent advances in artificial intelligence and machine learning for nonlinear relationship analysis and process control in drinking water treatment: A review. Chemical Engineering Journal 405, 126673

Liu, Q.-F. and Kim, S.-H. (2008) Evaluation of membrane fouling models based on bench-scale experiments: A comparison between constant flowrate blocking laws and artificial neural network (ANNs) model. Journal of Membrane Science 310(1), 393-401. https://doi.org/10.1016/j.memsci.2007.11.020

Mulder, M. (1999) Basic Principles of membrane technology, 2nd edition., Kluwer academic publisher.

Niu, C., Li, X., Dai, R. and Wang, Z. (2022) Artificial intelligence-incorporated membrane fouling prediction for membrane-based processes in the past 20 years: A critical review. Water Research 216, 118299. https://doi.org/10.1016/j.watres.2022.118299

Nthunya, L.N., Bopape, M.F., Mahlangu, O.T., Mamba, B.B., Van der Bruggen, B., Quist-Jensen, C.A. and Richards, H. (2022) Fouling, performance and cost analysis of membrane-based water desalination technologies: A critical review. Journal of Environmental Management 301, 113922

O'Reilly, G., Bezuidenhout, C.C. and Bezuidenhout, J.J. (2018) Artificial neural networks: applications in the drinking water sector. Water Supply 18(6), 1869-1887. 10.2166/ws.2018.016

Park, S., Baek, S.-S., Pyo, J., Pachepsky, Y., Park, J. and Cho, K.H. (2019) Deep neural networks for modeling fouling growth and flux decline during NF/RO membrane filtration. Journal of Membrane Science 587, 117164. https://doi.org/10.1016/j.memsci.2019.06.004

Piron, E., Latrille, E. and René, F. (1997) Application of artificial neural networks for crossflow microfiltration modelling: “black-box” and semi-physical approaches. Computers & Chemical Engineering 21(9), 1021-1030. https://doi.org/10.1016/S0098-1354(96)00332-8

Reid, R.C., Prausnitz, J.M. and Poling, B.E. (1987) The properties of gases and liquids. McGraw Hill Book Co., New York, NY.

Rudolph, G., Virtanen, T., Ferrando, M., Güell, C., Lipnizki, F. and Kallioinen, M. (2019) A review of in situ real-time monitoring techniques for membrane fouling in the biotechnology, biorefinery and food sectors. Journal of Membrane Science 588, 117221. https://doi.org/10.1016/j.memsci.2019.117221

Salinas-Rodriguez, S.G. (2011) Particulate and organic matter fouling of seawater reverse osmosis systems: Characterization, modelling and application, UNESCO-IHE PhD Thesis. CRC Press.

Salinas-Rodriguez, S.G., Amy, G.L., Schippers, J.C. and Kennedy, M.D. (2015) The Modified Fouling Index Ultrafiltration constant flux for assessing particulate/colloidal fouling of RO systems. Desalination 365, 79-91. https://doi.org/10.1016/j.desal.2015.02.018

Salinas-Rodríguez, S.G., Boerlage, S.F.E., Schippers, J.C., Kennedy, M.D., Salinas-Rodríguez, S.G., Schippers, J.C., Amy, G.L., Kim, I.S. and Kennedy, M.D. (2021) Seawater Reverse Osmosis Desalination: Assessment and Pre-treatment of Fouling and Scaling, p. 0, IWA Publishing.

Schippers, J.C. and Verdouw, J. (1980) The modified fouling index, a method of determining the fouling characteristics of water. Desalination 32, 137-148. https://doi.org/10.1016/S0011-9164(00)86014-2

Schmidhuber, J. (2015) Deep learning in neural networks: An overview. Neural Networks 61, 85-117. https://doi.org/10.1016/j.neunet.2014.09.003

Shi, Y., Wang, Z., Du, X., Gong, B., Jegatheesan, V. and Haq, I.U. (2021) Recent Advances in the Prediction of Fouling in Membrane Bioreactors. Membranes 11(6), 381

Teodosiu, C., Pastravanu, O. and Macoveanu, M. (2000) Neural network models for ultrafiltration and backwashing. Water Research 34(18), 4371-4380. https://doi.org/10.1016/S0043-1354(00)00217-7

Tian, J.-y., Ernst, M., Cui, F. and Jekel, M. (2013) Correlations of relevant membrane foulants with UF membrane fouling in different waters. Water Research 47(3), 1218-1228. https://doi.org/10.1016/j.watres.2012.11.043

Van Der Bruggen, B., Vandecasteele, C., Van Gestel, T., Doyen, W. and Leysen, R. (2003) A review of pressure-driven membrane processes in wastewater treatment and drinking water production. Environmental Progress 22(1), 46-56. https://doi.org/10.1002/ep.670220116

Vewin (2019) NL Drinking water fact sheet 2019. 0–1.

Viet, N.D. and Jang, A. (2021) Development of artificial intelligence-based models for the prediction of filtration performance and membrane fouling in an osmotic membrane bioreactor. Journal of Environmental Chemical Engineering 9(4), 105337. https://doi.org/10.1016/j.jece.2021.105337

Viet, N.D., Jang, D., Yoon, Y. and Jang, A. (2022) Enhancement of membrane system performance using artificial intelligence technologies for sustainable water and wastewater treatment: A critical review. Critical Reviews in Environmental Science and Technology 52(20), 3689-3719. 10.1080/10643389.2021.1940031

Villacorte, L.O., Ekowati, Y., Winters, H., Amy, G., Schippers, J.C. and Kennedy, M.D. (2015) MF/UF rejection and fouling potential of algal organic matter from bloom-forming marine and freshwater algae. Desalination 367, 1-10. https://doi.org/10.1016/j.desal.2015.03.027

Wu, S., Hua, X., Ma, B., Fan, H., Miao, R., Ulbricht, M., Hu, C. and Qu, J. (2021) Three-Dimensional Analysis of the Natural-Organic-Matter Distribution in the Cake Layer to Precisely Reveal Ultrafiltration Fouling Mechanisms. Environmental Science & Technology 55(8), 5442-5452. 10.1021/acs.est.1c00435

Xu, Y., Liu, X., Cao, X., Huang, C., Liu, E., Qian, S., Liu, X., Wu, Y., Dong, F. and Qiu, C.-W. (2021) Artificial intelligence: A powerful paradigm for scientific research. The Innovation 2(4)

Yuan, W. and Zydney, A.L. (2000) Humic Acid Fouling during Ultrafiltration. Environmental Science & Technology 34(23), 5043-5050. 10.1021/es0012366

Zhao, L., Dai, T., Qiao, Z., Sun, P., Hao, J. and Yang, Y. (2020) Application of artificial intelligence to wastewater treatment: A bibliometric analysis and systematic review of technology, economy, management, and wastewater reuse. Process Safety and Environmental Protection 133, 169-182. https://doi.org/10.1016/j.psep.2019.11.014

Zhao, Z.Q., Zheng, P., Xu, S.T. and Wu, X. (2019) Object Detection With Deep Learning: A Review. IEEE Transactions on Neural Networks and Learning Systems 30(11), 3212-3232. 10.1109/TNNLS.2018.2876865

Annex I - ANN modeling of membrane fouling in UF

Table AI.1 ANN modeling of membrane fouling characteristics in UF from literature (adapted from (Niu et al. 2022)

Membrane type	Inputs	Purpose/Outputs	Type	Performance	Reference
UF	pH, ionic strength and pressure	Permeate flux	MLP	Average error = 3.6%	(Richard Bowen et al., 1998)
UF	Permeate flow rate, pressure, temperature and turbidity	Fouling resistance	MLP	Error < 5%	(Delgrange et al., 1998a)
UF	Permeate flow rate, turbidity and temperature	TMP	RNN	RE = 3.9%	(Delgrange et al., 1998b)
UF	Turbidity, pH, DO, UV absorbency, TOC, etc.	Fouling resistance	RNN	RE < 10%	(Delgrange-Vincent et al., 2000)
UF	Time instants and initial flux value	Permeate flux after backwashing	MLP	RE = 3.8%	(Teodosiu et al., 2000)
UF	Bulk concentration, stirrer speed, pressure and time	Permeate flux and rejection	MLP	Average error = 3.6% (flux) Average error = 5.2% (rejection)	(Bhattacharjee and Singh 2002)
UF	TMP and time	Permeate flux, fouling resistance and rejection	MLP	Average error < 1%	(Razavi et al., 2003)
UF	Inlet pressure, filtration duration, turbidity, temperature and UV absorbency	Permeate flux	MLP	R^2 = 0.999	(Oh et al., 2004)
UF	TMP, feed concentration and time	Permeate flux and total soluble solid	MLP	Mean absolute errors = 1%	(Rai et al., 2005)
UF	TMP, filtration time, particle diameters, etc.	Permeate flux	MLP/RBF	MLP: R^2 = 0.958 RBF: R^2 = 0.988	(Sahoo and Ray 2006)
UF	Water turbidity and	Permeate flux	MLP	RE < 5%	(Curcio et al., 2006)

	bacteria concentrations				
UF	Particle size, solution pH and ionic strength	Permeate flux	RBF	$R^2 = 0.988$ RMSE = 0.082×10^{-5} m/s	(Chen and Kim 2006)
UF	Feed concentration, electric field, TMP and cross flow velocity	Permeate flux	MLP	RE = 1%	(Sarkar et al., 2009)
UF	Aggressivity of the cleaning protocol, time and number of operational cycle	Permeate flux	MLP	RMSE = 0.014 L/(m^2•h)	(Guadix et al., 2010)
UF	TMP, pH and feed concentration, etc.	Permeate flux and rejection	MLP	$R^2 = 0.929$ (flux)R^2 = 0.983 (rejection)	(Rahmanian et al., 2011)
UF	pH, feed concentration and surfactant to metal molar ratio	Permeate flux and rejection	MLP	$R^2 = 0.9254$ (flux) R^2 = 0.9813 (rejection)	(Rahmanian et al., 2012)
UF	Temperature, TMP, pH and cross-flow velocity	Permeate flux and fouling resistance	MLP	$R^2 = 0.9999$ (flux) $R^2 = 0.9999$ (resistance)	(Soleimani et al., 2013)
UF	Temperature, TMP, pH, time and crossflow velocity.	Permeate flux	MLP	$R^2 = 0.9999$	(Meighani et al., 2013)
UF	Temperature, pH, TMP, cross-flow velocity and time	Flux decline	MLP	R = 0.99997	(Badrnezhad and Mirza 2014)
UF	TMP, crossflow velocity and time	Permeation flux	MLP	$R^2 = 0.9977$	(Corbaton-Baguena et al., 2016)
UF	5 fluorescence spectral components for feed water organic constituents and pH, etc.	Fouling resistance	MLP	MAPE <5%	(Peleato et al., 2017)
UF	Surfactant-to-metal ratio, pH and	Permeate flux and rejection rate	MLP	$R^2 = 0.9974$	(Lin et al., 2017)

	cumulative sampling volume				

BP: back-propagation; MAPE: mean absolute percentage error; MLP: multilayer perceptron; NSRMSE: normalized square root of mean square error; R^2: determination coefficient; R: correlation coefficient; RE: relative error; RBF: radial basis function; RMSE: root mean squared error; TMP: transmembrane pressure; UF: ultrafiltration

Annex II - Water quality parameters and resistance for correlation analysis

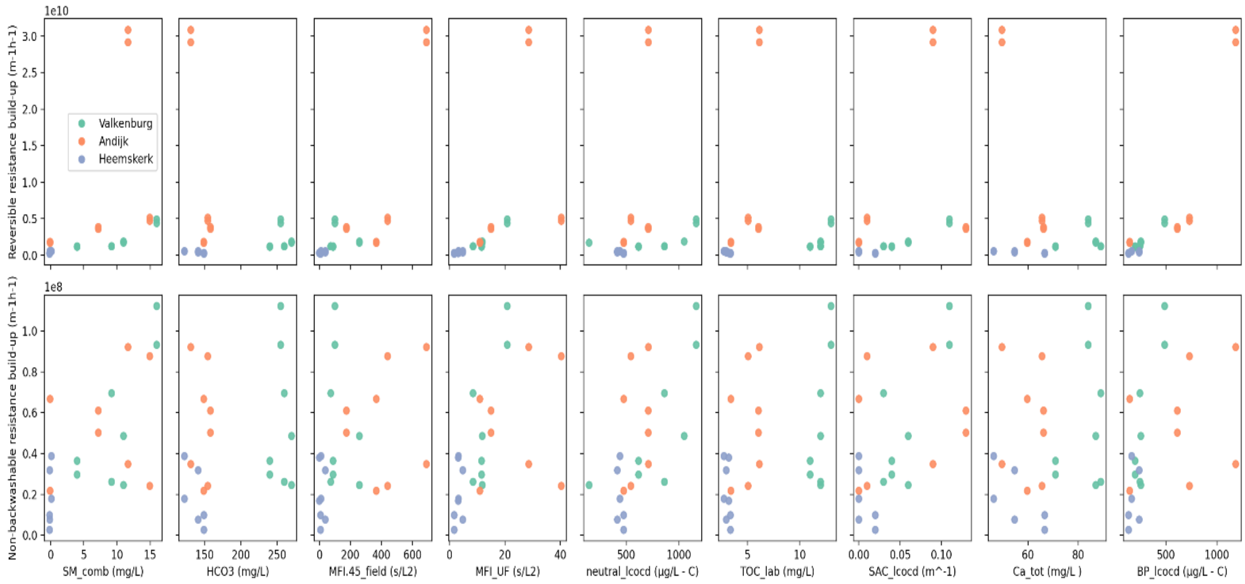

Figure 22 Overview of measured data points underlying the calculated correlation coefficients and significance numbers shown and discussed in the results & discussion section 4.1.3.

Annex III – Univariate Neural Network Models to Predict TMP

Table A3 1: Performance Metrics for all Neural Network Models Trained on Historical TMP data to predict the future values of TMP

Hidden Layer 1 (LSTM)	Hidden Layer 2 (Dense)	No. of trainable parameters	Training		Validation	
			RMSE (kPa)	R^2	RMSE (kPa)	R^2
16	16	1441	5.28	0.95	5.99	0.96
16	32	1729	4.75	0.96	6.12	0.96
16	**64**	**2305**	**4.83**	**0.96**	**5.79**	**0.96**
16	128	3457	4.82	0.96	5.80	0.96
32	16	4987	4.97	0.95	6.04	0.96
32	32	5441	4.99	0.95	6.20	0.96
32	64	6259	4.87	0.95	6.21	0.96
32	128	8705	4.53	0.96	6.02	0.96
64	16	17953	5.25	0.95	5.99	0.96
64	32	19009	4.87	0.96	5.87	0.96
64	64	21121	4.6	0.96	5.99	0.96
64	128	25345	4.7	0.96	6.04	0.96
128	16	68641	4.93	0.95	5.89	0.96
128	32	70721	6.9	0.91	8.85	0.91
128	64	74881	6.37	0.93	6.99	0.95
128	128	83201	4.53	0.96	6.49	0.95

Annex IV – Neural Network Models to Forecast Short-term increase in TMP over filtration cycles

Table A4 1: Performance of Different Neural Network Architectures When Forecasting Initial and Final TMP of 1 Filtration Cycle Ahead

Hidden Layer 1	Hidden Layer 2	1 Filtration Cycle Ahead			
		Train R^2		Validation R^2	
		Initial	Final	Initial	Final
16	16	0.95	0.95	0.49	0.55
16	**32**	**0.95**	**0.95**	**0.91**	**0.92**
16	64	0.95	0.95	0.90	0.88
16	128	0.95	0.95	0.68	0.65
32	16	0.95	0.95	0.91	0.91
32	32	0.95	0.95	0.88	0.90
32	64	0.95	0.95	0.76	0.86
32	128	0.95	0.95	0.88	0.90
64	16	0.95	0.95	0.89	0.89
64	32	0.95	0.95	0.90	0.87
64	64	0.95	0.95	0.88	0.87
64	128	0.95	0.95	0.91	0.92
128	16	0.95	0.95	0.91	0.91
128	32	0.95	0.95	0.81	0.94
128	64	0.94	0.94	0.92	0.90
128	128	0.95	0.95	0.91	0.91

Table A4 2: Performance of Different Neural Network Architectures When Forecasting Initial and Final TMP of 2 Filtration Cycles Ahead

Hidden Layer 1	Hidden Layer 2	1 Filtration Cycle Ahead				2 Filtration Cycle Ahead			
		Train R^2		Validation R^2		Train R^2		Validation R^2	
		Initial	Final	Initial	Final	Initial	Final	Initial	Final
16	16	0.99	0.99	0.96	0.93	0.95	0.94	0.90	0.84
16	32	0.99	0.99	0.87	0.94	0.95	0.94	0.87	0.90
16	64	0.99	0.99	0.95	0.94	0.95	0.95	0.92	0.91
16	128	0.97	0.96	0.73	0.81	0.92	0.92	0.85	0.80
32	16	0.97	0.96	0.80	0.88	0.91	0.93	0.92	0.91
32	32	0.99	0.99	0.97	0.97	0.94	0.94	0.91	0.92

32	64	0.99	0.99	0.97	0.96	0.95	0.95	0.93	0.92
32	128	0.99	0.99	0.95	0.94	0.95	0.95	0.90	0.89
64	16	0.99	0.99	0.98	0.98	0.95	0.94	0.94	0.93
64	32	0.99	0.99	0.98	0.97	0.95	0.95	0.92	0.93
64	64	0.99	0.99	0.97	0.95	0.95	0.94	0.91	0.93
64	128	0.99	0.99	0.98	0.97	0.95	0.95	0.94	0.93
128	16	0.99	0.99	0.92	0.95	0.95	0.95	0.88	0.91
128	32	0.99	0.99	0.97	0.96	0.95	0.94	0.93	0.93
128	64	0.99	0.99	0.90	0.95	0.95	0.94	0.93	0.93
128	128	0.99	0.99	0.97	0.91	0.95	0.95	0.94	0.93

Table A4 3: Performance of Different Neural Network Architectures When Forecasting Initial and Final TMP of 3 Filtration Cycles Ahead

Layer 1	Hidden Layer 2	1 Filtration Cycle Ahead				2 Filtration Cycle Ahead				3 Filtration Cycle Ahead			
		Train R^2		Validation R^2		Train R^2		Validation R^2		Train R^2		Validation R^2	
		Initial	Final	Initial	Final	Initial	Final	Initial	Final	Initial	Final	Initial	Final
16	16	0.99	0.99	0.95	0.96	0.94	0.93	0.91	0.89	0.94	0.94	0.92	0.91
16	32	0.99	0.99	0.94	0.95	0.94	0.93	0.88	0.88	0.94	0.94	0.88	0.88
16	64	0.99	0.99	0.94	0.93	0.94	0.94	0.91	0.87	0.94	0.94	0.90	0.90
16	128	0.99	0.99	0.94	0.94	0.94	0.94	0.90	0.89	0.94	0.94	0.88	0.86
32	16	0.99	0.99	0.85	0.77	0.94	0.94	0.86	0.79	0.95	0.94	0.84	0.79
32	32	0.99	0.99	0.96	0.97	0.94	0.94	0.92	0.92	0.94	0.94	0.93	0.92
32	64	0.99	0.99	0.96	0.94	0.94	0.94	0.92	0.92	0.94	0.94	0.92	0.91
32	128	0.93	0.89	0.92	0.87	0.85	0.79	0.88	0.87	0.87	0.86	0.89	0.89
64	16	0.99	0.99	0.95	0.97	0.94	0.94	0.90	0.93	0.94	0.94	0.89	0.88
64	32	0.97	0.97	0.91	0.91	0.93	0.92	0.88	0.90	0.93	0.93	0.91	0.86
64	64	0.99	0.99	0.96	0.91	0.94	0.94	0.91	0.93	0.94	0.94	0.94	0.92
64	128	0.99	0.99	0.80	0.85	0.94	0.94	0.91	0.92	0.95	0.94	0.91	0.84

128	16	0.99	0.99	0.97	0.97	0.94	0.94	0.91	0.91	0.94	0.94	0.90	0.91
128	**32**	**0.99**	**0.99**	**0.98**	**0.99**	**0.94**	**0.94**	**0.94**	**0.94**	**0.94**	**0.94**	**0.94**	**0.92**
128	64	0.94	0.96	0.98	0.98	0.92	0.92	0.93	0.93	0.92	0.89	0.91	0.91
128	128	0.99	0.99	0.98	0.98	0.94	0.94	0.93	0.93	0.94	0.94	0.94	0.93